

**ESTIMATING ROADSIDE ENCROACHMENT RATES
WITH THE COMBINED STRENGTHS OF ACCIDENT-
AND ENCROACHMENT-BASED APPROACHES**

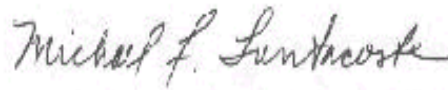
FINAL REPORT

Publication No. FHWA-RD-01-124

Shaw-Pin Miaou, Ph.D.
Safety and Structural Systems Division
Texas Transportation Institute
Texas A&M University System
College Station, Texas 77843-3135
(979) 862-8753
s-miaou@tamu.edu

FOREWORD

This report assesses the consistency of estimating vehicle roadside encroachment rates using accident-based prediction models. The research used two data sets developed from FHWA's Highway Safety Information System. These data are more recent than those reported in the previous assessments. By synthesizing the models developed from this and previous studies, a roadside encroachment rate estimation model was recommended. The model allows the encroachment rates to be estimated by average annual daily traffic volume, lane width, horizontal curvature, and vertical grade for rural two-lane undivided roads.



Michael F. Trentacoste
Director, Office of Safety
Research & Development

NOTICE

This document is disseminated under the sponsorship of the Department of Transportation in the interest of information exchange. The United States Government assumes no liability for its contents or use thereof. This report does not constitute a standard, specification, or regulation. The United States Government does not endorse products or manufacturers. Trade and manufacturers' names appear in this report only because they are considered essential to the object of the document.

1. Report No. FHWA-RD-01-124	2. Government Accession No.	3. Recipient's Catalog No.	
4. Title and Subtitle ESTIMATING ROADSIDE ENCROACHMENT RATES WITH THE COMBINED STRENGTHS OF ACCIDENT- AND ENCROACHMENT-BASED APPROACHES		5. Report Date September 2001	
		6. Performing Organization Code	
7. Author(s) S.P. Miaou		8. Performing Organization Report No.	
9. Performing Organization Name and Address Oak Ridge National Laboratory Attn: Pat Hu P.O. Box 2008 Bldg. 3156, MS-6073 Oak Ridge, TN 37831		10. Work Unit No. (TRAIS)	
		11. Contract or Grant No. DTFH61-94-Y-00107	
12. Sponsoring Agency Name and Address Federal Highway Administration Turner-Fairbanks Highway Research Center 6300 Georgetown Pike McLean, VA 22101-2296		13. Type of Report and Period Covered Final Report February 28, 1998 – September 21, 2001	
		14. Sponsoring Agency Code	
15. Supplementary Notes Contracting Officer's Technical Representative (COTR's): Joe Bared			
16. Abstract <p>In two recent studies by Miaou, he proposed a method to estimate vehicle roadside encroachment rates using accident-based models. He further illustrated the use of such method to estimate roadside encroachment rates for rural two-lane undivided roads using data from the Seven States Cross-Section Data Base of Federal Highway Administration [FHWA]. The results of his study indicated that the proposed method could be a viable approach to estimating roadside encroachment rates without actually collecting the encroachment data in the field, which can be expensive and technically difficult.</p> <p>This study tested the consistency of Miaou's approach using two data sets from FHWA's Highway Safety Information System (HSIS). In addition, by synthesizing the models developed from this and previous studies, a roadside encroachment rate estimation model was recommended. The model allows the rates to be estimated by average annual daily traffic volume, lane width, horizontal curvature, and vertical grade for rural two-lane undivided roads.</p>			
17. Key Word Roadside Encroachment, Roadway Geometric, Accident Prediction Model		18. Distribution Statement No restrictions. This document is available to the public through the National Technical Information Services, Springfield, VA 22161	
19. Security Classif. (of this report) Unclassified	20. Security Classif. (of this page) Unclassified	21. No. of Pages	22. Price

Metric Conversion Factors

Approximate Conversions to SI Units

Symbol	When You Know	Multiply By	To Find	Symbol
Length				
in	inches	25.4	millimeters	mm
ft	feet	0.305	meters	m
yd	yards	0.914	meters	m
mi	miles	1.61	kilometers	km
Area				
in ²	square inches	645.2	square millimeters	mm ²
ft ²	square feet	0.093	square meters	m ²
yd ²	square yards	0.836	square meters	m ²
ac	acres	0.405	hectares	ha
mi ²	square miles	2.59	square kilometers	km ²
Volume				
fl oz	fluid ounces	29.57	milliliters	ml
gal	gallons	3.785	liters	l
ft ³	cubic feet	0.028	cubic meters	m ³
yd ³	cubic yards	0.765	cubic meters	m ³
Mass				
oz	ounces	28.35	grams	g
lb	pounds	0.454	kilograms	kg
T	short tons (2000 lbs)	0.907	megagrams	Mg
Temperature (exact)				
°F	Fahrenheit temperature	5(F-32)/9 or (F-32)/1.8	Celsius temperature	°C
Illumination				
fc	foot-candles	10.76	lux	lx
fl	foot-Lamberts	3.426	candela/m ²	cd/m ²
Force and Pressure or Stress				
lbf	pound-force	4.45	newtons	N
psi	pound-force per square inch	6.89	kilopascals	kPa

TABLE OF CONTENTS

ESTIMATING ROADSIDE ENCROACHMENT FREQUENCIES USING MINNESOTA AND WASHINGTON DATA.....	1
Background	1
Models	2
A Recommended Encroachment Model	2
Table 1	4
Table 2.....	5
APPENDIX A – ESTIMATING VEHICLE ROADSIDE ENCROACHMENT FREQUENCIES USING ACCIDENT PREDICTION MODELS	7
Abstract	7
Introduction.....	8
A Run-off-the-Road Accident Prediction Model.....	11
The Proposed Method	14
Illustrations	16
Discussions	19
References	20
List of Tables	22
List of Figures	22
APPENDIX B – ANOTHER LOOK AT THE RELATIONSHIP BETWEEN ACCIDENT – AND ENCROACHMENT-BASED APPROACHES TO RUN-OF-THE-ROAD ACCIDENTS MODELING.....	29
Abstract	29
Introduction.....	31
Encroachment-Based Thinking.....	35
Form of Mean Functions.....	51
Estimating Encroachment Rates	57
Discussion.....	66
References	68
List of Tables	70
List of Figures	70
APPENDIX C – RESEARCH STATEMENT: ESTIMATING ROADSIDE ENCROACHMENT RATES WITH THE COMBINED STRENGTHS OF ACCIDENT- AND ENCROACHMENT-BASED APPROACHES	83
Background	83
Proposed Research Plan.....	86
Proposed Tasks	87
References	88

ESTIMATING ROADSIDE ENCROACHMENT FREQUENCIES USING MINNESOTA AND WASHINGTON DATA

BACKGROUND

The problem statement on which this study was based is presented in Appendix C. The two-lane road-segment data used in this study are provided by Dr. Andrew Vogt as part of his study presented in Vogt, A. and Bared, J.G., *Accident Models for Two-Lane Rural Roads: Segments and Intersections*, FHWA-RD-98-133, Federal Highway Administration, October 1998. Detailed background information of the two data sets and associated descriptive statistics of key traffic and design variables can be found in Vogt and Bared's report. On the accident data, this study focuses on run-off-the-road accidents, while Vogt and Bared considered total number of accidents on these road segments, both on mainline and roadside. Their analysis also examined accident-flow-design relationships for accidents at different severity levels.

In this study, only road segments with average annual daily traffic (ADT) less than 12,000 and with all horizontal curvatures within a segment less than 30 degrees were selected for modeling. As a result, 32 out of 712 road segments in Washington and 11 out of 619 in Minnesota were removed from the data sets before the analysis.

The modeling concepts and encroachment frequency estimation procedures are contained in Appendices A and B. The negative binomial (NB) models used in this study are generalized version of the models described in Appendix B and in Vogt and Bared [1998]. The models allow interactive effects among variables with multiple values within a segment.

After some examinations of the range of variations of key design variables included in the two data sets, it was concluded that Minnesota data did not have the data required for the study. Specifically, there are almost no road segments in the Minnesota data that have roadside hazard rating greater than or equal to six. Recall that for the approach described in Appendices A and B to work properly, it is required that a significant percentage of the road segments in the data set needs to have very "bad" roadside conditions.

Washington data, on the other hand, seemed to have the data needed for the study. Another strength of the Washington data, relative to the Minnesota data, is that the data set contains more recent accident and roadway data (from 1993 to 1995), while the Minnesota data contain older data from 1985 to 1989.

MODELS

Both data sets were modeled extensively, including numerous experiments with different functional forms and variable categorization schemes. The best models are presented in Table 1. For the reason stated above, the model developed from the Washington data was used as the primary model for estimating the roadside encroachment frequency, while the Minnesota model, as well as the models presented in Appendices A and B, were used as reference models to strengthen the Washington model when appropriate.

A RECOMMENDED ENCROACHMENT MODEL

Following the concept presented in Appendix A, we recommend the following model be used to estimate the expected frequency of roadside encroachments by ADT, lane width, horizontal curvature, and vertical grade for rural two-lane roads. Note that some subjective judgments were injected in the selection and synthesis of the recommended model.

$$E = (365 \times ADT / 1000000) \times \exp(\mathbf{b}_{st} - 0.04 \times ADT / 1000 + Ln f + Hazf + 0.12 \times HC + 0.05 \times VG)$$

where

E = expected number of roadside encroachments per mile per year.

ADT = average annual daily traffic (in number of vehicles) from 1,000 to 12,000.

\mathbf{b}_{st} = State constant with a default value of -0.42 . For those areas (or States) where rural two-lane roads data are available, it is recommended that \mathbf{b}_{st} be estimated as the natural log of the run-off-the-road accident rate for road segments with low ADT (e.g., < 2000) that are relatively straight (e.g., horizontal curvature < 3 degrees) and leveled (e.g., vertical grade $< 3\%$).

$Lnf = 0, 0.20, \text{ and } 0.44$, respectively, for road segments with 12 ft, 11ft, and 10 ft wide lane.

$Hazf = 0.4 \text{ to } 0.5$ (with a default value of 0.45).

$HC = \text{horizontal curvature (in degrees per 100 ft arc) from 0 to 30 degrees.}$

$VG = \text{vertical grade (in percent) from 0 to 10 percent.}$

Using the default values for b_{st} and $Hazf$, example estimates of roadside encroachment frequencies are given in Table 2. Of course, those example estimates in the table where $HC = 30$ and $VG = 10$ are extreme design scenarios that do not actually exist in any of the data sets used in this and earlier studies and are therefore not as reliable.

Table 1. Estimated regression coefficients of an extended negative binomial regression model and associated statistics for single-vehicle run-off-the-road accidents.

Covariate	Washington	Minnesota
	Estimated Parameter Value	Estimated Parameter Value
= Dummy intercept (=1)	- 0.4186 (±0.14; -2.95)	-0.16165 (±0.32; -0.51)
= AADT per lane (in 10 ³)	-0.0836 (±0.03; -2.33)	-0.068571 (±0.06; -1.15)
= 1 if lane width (in ft) is 10 ft or less	0.4379 (±0.18; 2.41)	-----
= 1 if lane width (in ft) = 11 or 12 = 0 otherwise	-----	-0.46397 (±0.19; -2.45)
=1 if lane width (in ft) =12 =0 otherwise	-----	-0.12982 (±0.13; -1.00)
= Shoulder width (in ft per side)	-0.0496 (±0.02; -2.51)	-0.16318 (±0.03; -6.35)
= 1 if Roadside Hazard Rating is greater than or equal to 4 = 0 otherwise	0.1754 (±0.10; 1.66)	-----
= 1 if Roadside Hazard Rating is greater than or equal to 6 = 0 otherwise	0.1348 (±0.13;1.06)	-----
= 1 if Roadside Hazard Rating is greater than or equal to 3	-----	0.00797 (±0.12; 0.07)
= Driveway density (No. of driveways per mi) (Note: Max density is limited to 50)	NS	-0.02292 (±0.01; -2.14)
Percent of commercial trucks	NS	0.00745 (±0.013; 0.58)
Horizontal curvature (in degree/100 ft arc)	0.1197 (±0.02; 5.56)	0.10620 (±0.027; 3.87)
Vertical grade (in percent)	0.0154 (±0.03; 0.46)	0.25024 (±0.056; 4.44)
No. of road segments	680	608
Dispersion parameter of the NB model (a)	0.346 (±0.067; 5.22)	0.31765 (±0.090; 3.54)
R ² _α (Overdispersion-Based R-Square Measure)	0.80	0.87
Expected vs. observed total number of accidents	940 vs 941	524.5 vs 526.0

Data Source: Vogt A. and Bared, J.G., Accident Models for Two-Lane Rural Roads: Segments and Intersections, FHWA-RD-98-133, Federal Highway Administration, October 1998.

Data Screening: Only road segments with average annual daily traffic less than 12,000 and with all horizontal curvatures within a segment less than 30 degrees were selected. As a result, 32 and 11 road segments from Washington and Minnesota, respectively, were removed from the data sets.

Notes: (1) Values in parentheses are asymptotic standard deviation and t-statistics of the coefficients above.

(2) ----- indicates "not included in the model;" NS stands for "not significant statistically."

(3) 1 mile = 1.61 km, 1 ft = 0.3048 m.

Table 2. Examples of estimated number of encroachments by ADT, lane width, horizontal curvature, and vertical grade.

ADT (# of Vehicles)	Lane Width (FT)	H. Curvature (Deg/100 ft Arc)	Vertical Grade (Percent)	Encroachments (per mile per year)
1000	12	0	0	0.36
2000	12	0	0	0.69
3000	12	0	0	1.00
4000	12	0	0	1.28
5000	12	0	0	1.54
6000	12	0	0	1.78
7000	12	0	0	1.99
8000	12	0	0	2.18
9000	12	0	0	2.36
10000	12	0	0	2.52
11000	12	0	0	2.66
12000	12	0	0	2.79
1000	11	3	2	0.70
2000	11	3	2	1.34
3000	11	3	2	1.94
4000	11	3	2	2.48
5000	11	3	2	2.98
6000	11	3	2	3.43
7000	11	3	2	3.85
8000	11	3	2	4.23
9000	11	3	2	4.57
10000	11	3	2	4.88
11000	11	3	2	5.16
12000	11	3	2	5.40
1000	10	30	10	33.86
2000	10	30	10	65.06
3000	10	30	10	93.76
4000	10	30	10	120.11
5000	10	30	10	144.25
6000	10	30	10	166.32
7000	10	30	10	186.43
8000	10	30	10	204.71
9000	10	30	10	221.27
10000	10	30	10	236.21
11000	10	30	10	249.64
12000	10	30	10	261.66

APPENDIX A

ESTIMATING VEHICLE ROADSIDE ENCROACHMENT FREQUENCIES USING ACCIDENT PREDICTION MODELS

Shaw-Pin Miaou
Center for Transportation Analysis, Energy Division
Oak Ridge National Laboratory
P.O. Box 2008, MS 6073, Building 3156, Oak Ridge, TN 37831, USA
Phone: (423) 574-6933, Fax: (423) 574-3851; E-Mail: PNI@ORNL.GOV

July 1996

Revised November 1996 and March 1997

Published in *Transportation Research Record 1599*, Transportation Research Board, National Research Council, pp. 64-71, September 1997.

ABSTRACT

The existing data to support the development of roadside encroachment-based accident prediction models are limited and largely outdated. Under the sponsorship of the Federal Highway Administration and Transportation Research Board, several roadside safety projects have attempted to address this issue by proposing rather comprehensive data collection plans and conducting pilot data collection efforts. It is clear from these studies that the required cost for the proposed roadside field data collection efforts will be very high. Furthermore, the validity of any field-collected roadside encroachment data may be questionable because of the technical difficulty to distinguish intentional (or controlled) from unintentional (or uncontrolled) encroachments. This paper proposes a method to estimate some of the basic roadside encroachment parameters, including vehicle roadside encroachment frequency and the probability distribution of lateral extent of encroachments, using existing accident-based prediction models. The method is developed by utilizing the probabilistic relationships between a roadside encroachment event and a run-off-the-road accident event. With some assumptions, the method is capable of providing a wide range of basic encroachment parameters from conventional accident-based prediction models. To illustrate the concept and use of such a method, some basic encroachment parameters are estimated for rural, two-lane, undivided roads. In addition, the estimated encroachment parameters are compared with those estimated from the existing encroachment data. The illustration shows that the method described in this paper can be a viable approach to estimating basic encroachment parameters of interest and, thus, has the potential of reducing the roadside data collection cost.

Key Words: Run-Off-the-Road Accident, Vehicle Roadside Encroachment, Roadside Design, Accident Prediction Model

ESTIMATING VEHICLE ROADSIDE ENCROACHMENT FREQUENCIES USING ACCIDENT PREDICTION MODELS

INTRODUCTION

Past research on the safety of roadside environment has produced more-forgiving roadside hardware and improved roadside design practices (1). However, the latest national statistics still indicate that about one-third of the fatal traffic crashes are associated with vehicles running off the road (2). For example, 10,473 out of 34,928 fatal traffic crashes that occurred in 1992 were related to collision with roadside fixed objects and, in addition, a large percentage of the 3,281 fatal rollover crashes occurred on sideslopes and ditches. These statistics on run-off-the-road accidents (RORA) continue to indicate the need for more research to develop cost-effective road-driver-, and vehicle-related countermeasures to reduce the frequency and consequences of such accidents (3,4).

To develop cost-effective road-related countermeasures, one needs to have a good understanding of the relationship between roadside safety and roadside design. To date, much of what is known about the roadside safety-design relationships remains to be either qualitative in nature or dependent on subjective engineering guesses (4,5). Recent studies have suggested that new and cost-effective analysis approaches and data collection efforts are essential if a more objective basis of such relationships is to be developed (6-8).

Models used in previous studies to develop the relationships between the RORA frequency, traffic flows, and roadside hazards, such as embankments, utility poles, trees, luminaries, guardrail, and median barriers, have been categorized as either an accident-based approach or an encroachment-based approach (5). The first approach uses statistical regression models to develop the relationships, in which the RORA frequency of hitting a particular or a combination of roadside hazards is the dependent variable, and traffic flows, roadway mainline designs, roadside designs, and other variables are the explanatory variable (or covariates). For example, in one of the models developed in Zegeer et al. (9), single vehicle (SV) RORA frequencies, including fixed-object and rollover accidents, were regressed over average annual daily traffic (AADT), lane width, shoulder width, clear roadside recovery distance (CRRD), and terrain type, where CRRD is a summary measure of the width of the flat, unobstructed, and smooth area

adjacent to the outside edge of the shoulder within which there is a reasonable opportunity for the safe recovery of an out-of-control vehicle. In another study by Zegeer et al. (10), RORA frequencies hitting various types of roadside fixed objects such as utility poles, trees, guardrails, were regressed over AADT, lane width, and density and lateral offset of the object. The models so developed are typically referred to as accident-based accident prediction models. It should be noted, however, that Zegeer et al.'s studies have heavily relied on the use of lognormal regression models. More appropriate accident prediction models based on the Poisson and negative binomial (NB) regression models have been advocated and widely used in recent years (e.g., 11-15). Also, note that, except the two studies described above, data on roadside variables (excluding shoulder width and shoulder type) were, however, unavailable in most of these recent studies.

The second approach uses a series of conditional probabilities to describe the sequence of events resulting in a roadside accident. For example: (i) an errant vehicle leaves the traveled way and encroaches on the shoulder; (ii) the location of encroachment is such that the path of travel is directed towards a potentially hazardous roadside object; (iii) the hazardous object is sufficiently close to the travel lanes that control is not regained before encounter or collision between vehicle and object; and (iv) the collision is sufficiently severe enough to result in an accident of some level of severity. These types of models have traditionally been called roadside encroachment-based accident prediction models (1,5,16). The idea of the encroachment-based approach was to formulate and estimate each of these conditional probabilities based on traffic flow theory, geometry, vehicle dynamics, driver's behavior, and probability theory. Appendix F of the Transportation Research Board's Special Report 214 (SR214) (1) provides a good description of the encroachment model and its application on two-lane undivided roads. A recent review of such an approach and its relationship with the accident-based approach is given in Miaou (15).

During the last 30 years, there has been a constant effort to develop and refine the encroachment-based models. More recent plans and efforts to further improve roadside encroachment models include Mak and Sicking (6) and the National Cooperative Highway Research Program (NCHRP) Project 22-9 that is currently being conducted by Texas Transportation Institute (TTI), Texas A&M University.

Despite these efforts, the encroachment-based approach has been criticized as being full of subjective assumptions and lacking empirical basis or supporting data (5). For example, on each road section, the most basic parameters required by an encroachment-based model are the *vehicle roadside encroachment frequency* and the *probability distribution of lateral extent of encroachments* when roadside encroachments occur. The encroachment frequency is expected to vary from one road section to another, depending on roadway class, AADT, lane width, horizontal curvature, vertical grade, etc., while the probability distribution of lateral extent of encroachments is expected to vary by sideslope and other roadside design factors. At present, the existing parameters for developing encroachment-based models were estimated from data that are largely outdated (5,6,8). In addition, these data were collected on a small number of road sections and for a limited time period in a year, e.g., during winter or summer months. The Federal Highway Administration (FHWA) and Transportation Research Board (TRB) have been addressing the requirements and collection of such data through their sponsorship of several roadside safety projects. As a result, rather comprehensive data collection plans and pilot data collection efforts have been reported in Mak and Sicking (6), a recent interim report prepared for the NCHRP Project 17-11 (8), and Daily et al. (5). A review of these plans and pilot data collection results suggests that the cost of collecting the required roadside field data will be very high. Furthermore, the validity of any field collected encroachment data may be questionable because of the technical difficulty of distinguishing intentional (or controlled) from unintentional (or uncontrolled) encroachments.

This paper proposes a method for estimating the basic roadside encroachment parameters using the existing accident-based prediction models without actually collecting the data to estimate them. The method is developed by exploring the probabilistic relationships between a roadside encroachment event and a RORA event. With some assumptions, the method is capable of providing a wide range of basic encroachment parameters from conventional accident-based models. To illustrate the concept and use of such a method, the basic encroachment parameters are estimated for rural, two-lane, undivided roads. In addition, the estimated encroachment parameters are compared with those estimated from the existing encroachment data.

Section 2 of this paper illustrates of the proposed method, a rural two-lane road accident-based model, which was developed in Miaou (15). Since the theory behind the accident-based models

has been described quite extensively in many recent publications (e.g., *11-15*), the readers are referred to these publications for a review of the Poisson and NB regression-based accident prediction modeling theories. Section 3 describes the proposed method and its assumptions. Section 4 illustrates the concept and use of the proposed method by utilizing the accident-based model presented in Section 2. Some discussions on the potential extensions of such a method are provided in the last section.

In the following discussion, a “roadside encroachment” is said to occur when an errant vehicle crosses the outside edges of the travelway and encroaches on the shoulder, including both inside and outside shoulders. Thus, for a two-lane undivided road that has no inside shoulder, the total number of roadside encroachments includes departures of vehicles from near-side and far-side edges of the travelway in both directions. It is also important to note that roadside encroachments refer only to “unintentional or uncontrolled encroachments.” In other words, the “intentional or controlled encroachments” as a result of vehicles intentionally driven outside of the travel lane on, e.g., adjacent lane (in the same or opposite direction), shoulders, and traversable medians, are not counted as encroachments.

A RUN-OFF-THE-ROAD ACCIDENT PREDICTION MODEL

Run-off-the-road accidents and roadway data for rural, two-lane, undivided roads from a roadway cross-section design data base (*17*) administered by FHWA and TRB were used by Miaou (*15*) to develop an accident-based model. One important feature of this particular data base is that it contains a rather detailed description of key design elements of various roadside obstacles. The roadway data used in this study include traffic and geometric design data of 596 road sections in three States—Alabama, Michigan, and Washington. The total length of these sections is 1,788 mi (2,878 km). Except Alabama, every State has about 5 years of SV RORA data from 1980 to 1984 available for analysis. Alabama has about 2.5 years of accident data, but accidents that occurred in icy or snowy conditions were not recorded (*17*). Note that the data are not broken down by year. During the period considered, there were 4,632 SV reported to be involved in RORA on these road sections, regardless of vehicle and accident severity type. With the total vehicle miles estimated to be 7,639 million vehicle miles (12,299 million vehicle kilometers), the overall SV RORA rate was 0.61 SV RORA per million vehicle miles (0.38 SV RORA per million vehicle kilometers). A similar data set has been used in Zegeer et al. (*9*) to

evaluate the effect of sideslope on the rate of SV RORA. Detailed description and statistics of these road sections can be found in Rodgman et al. (17) and Zegeer et al. (9).

In addition to vehicle miles traveled, the covariates considered for individual road sections are presented in Table 1. They include (i) dummy variables for Michigan and Washington to capture the overall difference in SV RORA rate among States, due to differences in omitted variables such as weather, socioeconomic and geographic variables, accident reporting threshold, and underreporting rate; (ii) AADT per lane, used as a surrogate measure for traffic density; (iii) lane width; (iv) median clear roadside recovery distance, measured from the right edge of the shoulder; (v) paved shoulder width; (vi) earth, grass, gravel, or stabilized shoulder width; (vii) median sideslope from field measurements; (viii) terrain type, used as a surrogate measures for horizontal curvature and vertical grade; (ix) posted speed limit; (x) number of intersections per mile; (xi) number of driveways per mile; and (xii) number of bridges per mile. Many of these covariates were also considered by Zegeer et al. (9). Horizontal curvature and vertical grade data were not used in this exercise because 147 sections (about 25 percent) were found to have no curvature data, and 341 sections (about 57 percent) did not have grade information.

The NB regression model, as described in Miaou (13, 15), was employed, and the estimated parameters as well as their associated standard deviations and t-statistics are presented in Table 1. All covariates in the model have the expected effects. Discussions on the choice of covariates and the model's goodness-of-fit can be found in Miaou (15). About 62 percent of the "explainable variance" were explained by the covariates included in this model. It was suggested that a higher explanatory power might be achieved if horizontal curvature, vertical grade, and yearly data were available. Note that there is an ongoing research effort by the author attempting to enhance this model.

Posted speed limit was not found to be significant because of the lack of variation; 530 out of the 596 sections had a posted speed limit of 55 mph (89 kph). Although the number of intersections per mile had the expected effect, it was not found to be statistically significant (at a 20 percent a level) and was removed from the final model.

Major findings from the model are:

- If all considered variables have the same values, Michigan has the highest SV RORA rate, and Alabama has the lowest rate. Michigan's rate is about 20 percent higher than Washington because of the difference in weather, socioeconomic, and other factors, while Alabama is about 34 percent lower than Washington because of the incomplete Alabama accident data and differences in weather and other factors.
- AADT per lane shows a negative effect. Although many explanations have been offered in the literature as to why the effect is negative, one additional, plausible explanation is that all else being equal, higher vehicle density results in higher multiple-vehicle (MV) accident rate and lower SV accident rate.
- All else being equal, increasing lane width is expected to reduce SV RORA rate. Figure 1 gives an illustration of the expected SV RORA rates for various lane widths and sideslopes from the model.
- The effect of paved shoulder width was not found to be significantly different from the effect of the stabilized shoulder width. All else being equal, increasing shoulder width by 1 ft (0.3048 m) is expected to reduce SV RORA rate by about 9 percent. To give an example of how this reduction factor is typically used, let's consider a road section with zero shoulder width. By increasing the shoulder width from 0 to 11 ft (3.35 m), the SV RORA rate of this road section is expected to become: $(\text{SV RORA rate of the road section with no shoulder}) \times (1-0.09)^{11} = 0.35 \times (\text{SV RORA rate of the road section with no shoulder})$. If the SV RORA rate for the section with no shoulder is expected to be high, then 35 percent of this rate should still be quite significant. Note that a statistical discussion of this reduction factor can be found in Miaou and Lum (18).
- Steeper sideslope is associated with higher SV RORA rate. Figure 2 shows the relative rates for various sideslope ratios when compared to the rate of a sideslope of 7:1. The t-statistic of the estimated parameter in Table 1 shows that the sideslope was not as well determined statistically as other variables. One possible reason is that for each road section the median (i.e., 50th percentile) sideslope measurement was used as the most representative sideslope, but the actual sideslope may vary considerably within a given section (9).
- As expected, all else being the same, higher numbers of driveways and bridges per mile result in higher SV RORA rates.

In the next section, this model will be used to illustrate how an accident prediction model can be used to estimate roadside encroachment frequency and to derive the probability distribution of lateral extent of encroachment when encroachment occurs.

THE PROPOSED METHOD

The relationship between SV RORA probability and SV roadside encroachment probability for a vehicle traveling through a 1-mi or 1-km road section can be mathematically expressed as follows:

$$\begin{aligned}
 P(SV \text{ RORA} | \text{Mainline}, \text{Rdside Design}) &= P(\text{Rdside Encro} | \text{Mainline}, \text{Rdside Design}) \times \\
 &P(SV \text{ RORA} | \text{Rdside Encro}, \text{Mainline}, \text{Rdside Design}) \\
 &P(\text{No Rdside Encro} | \text{Mainline}, \text{Rdside Design}) \times \\
 &P(SV \text{ RORA} | \text{No Rdside Encro}, \text{Mainline}, \text{Rdside Design}) \\
 &= P(\text{Rdside Encro} | \text{Mainline}, \text{Rdside Design}) \times \\
 &P(SV \text{ RORA} | \text{Rdside Encro}, \text{Mainline}, \text{Rdside Design})
 \end{aligned} \tag{1}$$

where

Mainline = Mainline traffic and geometric design variables;

Rdside Design = Rdside design variables;

$P(SV \text{ RORA} | \text{Mainline}, \text{Rdside Design})$

= conditional probability of being involved in a SV RORA when a vehicle travels through a 1-mi or 1-km road section that has a given geometric design and traffic characteristics as described in *Mainline* and *Rdside Design*; (Note that it is assumed here that the probability of having more than one SV RORA by a vehicle is zero);

$P(\text{Rdside Encro} | \text{Mainline}, \text{Rdside Design})$

= conditional probability of having a SV roadside encroachment when a vehicle travels through a 1-mi or 1-km road section that has a given geometric design and traffic characteristics as described in *Mainline* and *Rdside Design*; (Note that it is assumed here that the probability of having more than one SV roadside encroachment by a vehicle is zero);

$P(SV \text{ RORA} | \text{Rdside Encro}, \text{Mainline}, \text{Rdside Design})$

= conditional probability of being involved in a SV RORA when a vehicle travels on a 1-mi or 1-km road section that has a given geometric design and traffic characteristics as described in *Mainline* and *Rdside Design* and has encroached on the roadside.

$P(\text{No Rdside Encro} / \text{Mainline}, \text{Rdside Design})$

= conditional probability of having no SV roadside encroachment when a vehicle travels through a 1-mi or 1-km road section that has a given geometric design and traffic characteristics as described in *Mainline* and *Rdside Design*; and

$P(\text{SV RORA} / \text{No Rdside Encro}, \text{Mainline}, \text{Rdside Design})$

= conditional probability of being involved in a SV RORA when a vehicle travels on a 1-mi or 1-km road section that has a given geometric design and traffic characteristics as described in *Mainline* and *Rdside Design* and has not encroached on the roadside (note that this probability is equal to zero).

One of the basic assumptions in the conventional encroachment-based models is that *Rdside Design* has a very small and negligible effect on roadside encroachment probability. Under this assumption, Equation (1) can be rewritten as:

$$P(\text{SV RORA} / \text{Mainline}, \text{Rdside Design}) = P(\text{Rdside Encro} / \text{Mainline}) \times P(\text{SV RORA} / \text{Rdside Encro}, \text{Mainline}, \text{Rdside Design}) \quad (2)$$

Note that even though the validity of this basic assumption may be debatable, it is not the intent of this paper to challenge any assumption used by the encroachment-based models.

Now, let's picture a condition where there exists an extremely bad roadside design such that when a vehicle encroaches on the roadside at any point on the road section it is 100 percent sure that the vehicle will result in a RORA. For example, one can picture a road section that has no shoulders and a ditch with a 1:1 sideslope ratio built right next to the traveled lane. Note that very dense point objects, such as trees and utility poles along the roadside, would also be good examples. Of course, a road section with such a bad roadside design may not exist in the sample. Thus, in practice, extrapolations beyond the range provided by the sample may be required. The reasonableness of the extrapolations depends on the extent of the extrapolation and functional relationship in question (e.g., whether it is linear or nonlinear). Note that some engineering and statistical judgments are required if a rather far-out extrapolation is required and the functional relationship appears to be nonlinear.

Under such a bad roadside design condition, $P(SV\ RORA/Rdside\ Encro,\ Mainline,\ "extremely\ bad"\ Rdside\ Design) = 1$, and therefore Equation (2) can be reexpressed as:

$$P(SV\ RORA / Mainline , " Extremely\ Bad " Rdside\ Design) = P(Rdside\ Encro / Mainline) \quad (3)$$

To estimate the expected annual number of RORA on a road section with R miles, one can simply multiply Equation (3) with $(V \times R)$, where V is the total number of vehicles traveling through the section per year ($=365HAADT$). That is,

$$P(SV\ RORA / Mainline , " Extremely\ Bad " Rdside\ Design) \times V \times \ell = P(Rdside\ Encro / Mainline) \times V \times \ell \quad (4)$$

In Equation (4), the right-hand side is an estimate of the annual roadside encroachment frequency of interest, and the left-hand side is an estimate of the expected number of SV RORA per year, which can be obtained from a conventional accident-based prediction model such as the one presented in the last section.

ILLUSTRATIONS

To estimate the roadside encroachment frequency using the model presented in Table 1, an extremely bad roadside design condition can be created by setting shoulder width = 0, median clear roadside recovery distance = 0, and median sideslope = 1. (Note that sideslope ratio of 1:1 is the maximum median sideslope recorded in the sample sections.) Except lane width and

AADT, other variables were set equal to their average values. Also, because Alabama has incomplete accident data, only Michigan and Washington models are used. Figure 3 shows the estimated roadside encroachment frequencies per mile per year by various lane widths and AADT's using Equation (4) under the described bad roadside conditions. The encroachment frequencies collected by Hutchinson and Kennedy (19) and Cooper (20), and the estimates given in SR214 based on an encroachment-based model are also presented in the figure for comparison.

One important observation from Figure 3 is that the estimated encroachment frequencies are very compatible with the encroachment data collected by others. Note that the encroachment frequencies reported in SR214 are higher than they should be for the following reason: An ad hoc ordinary least squares procedure was used for parameter estimation after log-transformations have been taken. Essentially, the procedure overlooked an important adjustment factor as described in Miaou and Lum (12). In addition, validation test results provided in the SR214 indicated that the predicted accident rate from the model developed in SR214 exceeded actual rates by up to 160 percent.

Several comments can be made about this proposed approach of estimating roadside encroachment frequency:

- One advantage of such an approach is that the encroachment frequency can be estimated for all kinds of mainline design and traffic conditions. For example, if horizontal curvature and vertical grade were included in the accident prediction model presented in Section 2, the encroachment frequencies could be estimated for various horizontal curvatures and vertical grades as well. To actually collect such detailed encroachment data will be very expensive and may be impractical.
- It has been suggested “the encroachment frequency estimated in this manner can only be as accurate as the accident data used as input.”(5) The suggestion is mainly related to the concern about the underreporting of minor accidents. This author would like to point out that this concern is not particularly serious for the approach proposed in this paper. The reason is that under the “extremely bad” roadside design condition stated above, the resulting RORA is expected to be very severe, and underreporting of such accidents is very unlikely. Therefore, provided a flexible mean functional form is used in developing

accident prediction models, the encroachment frequency estimated from such an approach is relatively unaffected by the underreporting of accidents.

- Another advantage of such an approach is that the estimated encroachment frequency is relatively uncontaminated by intentional encroachments. Again, the reason is that intentional encroachments are not likely to occur under such a bad roadside design condition.

It is important to point out that indeed a small extrapolation is used in the estimation because the assumed extreme roadside conditions, i.e., shoulder width = 0, median clear roadside recovery distance = 0, and median sideslope = 1, do not exist in the sample road sections. Note that for the sample road sections considered in this study, there are some sections that have shoulder width = 0, some that have median clear roadside recovery distance = 0, and some with median sideslope = 1, but there is no road section that has all three features combined. Thus, it is in this sense that the extrapolation is made.

It is expected that the estimated encroachment frequency represents only potentially harmful and unintentional encroachments (which are what the encroachment-based models need). As a result, the estimate is expected to be lower than what would actually happen on the roads, especially for those roads with wide shoulders where drivers tend to be more relaxed and harmless, and unintentional roadside encroachments do occur quite often.

Another possible use of such an approach is to estimate the probability of the lateral extent of encroachment when a roadside encroachment occurs. That is, given a roadside encroachment has occurred, the approach can be used to estimate the probability that the encroached vehicle, in the absence of roadside obstacles, will leave the traveled lane by at least a distance of, say, L , when encroaching on a relatively flat roadside. Conceptually, this estimate can be achieved by a simple extension of the approach described above. Specifically, it can be achieved by setting shoulder width = L , median clear roadside recovery distance = 0, and median sideslope = 1. The other variables can be set in exactly the same way. Mathematically, Equations 2 and 3 can be modified to include the shoulder width (SW) explicitly as follows:

$$P(SV RORA / Mainline, SW = L \text{ Other Rdside Design}) = P(Rdside Encro > L / Mainline) \times P(SV RORA / Rdside Encro > L, Mainline, SW = L, \text{ Other Rdside Design})$$

(5)

$$P(SV RORA / Mainline, SW = L, \text{ "Extremely Bad" Other Rdside Design}) = P(Rdside Encro > L / Mainline)$$

(6)

Figure 4 shows a derived probability distribution of the lateral extent of encroachments using such approach. Since shoulder width is used to estimate the probability, the distribution is good for leveled or flat roadside conditions with no slopes. This estimated distribution can be seen to be quite consistent with AASHTO's distributions for roads with a design speed of 50-60 mi/h (80-96 km/h). On the other hand, it is very different from the distributions derived from Hutchinson and Kennedy's encroachment data. Note that, as pointed out by Daily et al. (5), the basis of AASHTO's distributions is not clear from its *Roadside Design Guide*. In addition, the estimation of a single distribution for a design speed has been controversial; it has been suggested that multiple distributions for different sideslope ratios are necessary. In theory, this distribution could be conditional on sideslope, shoulder type (e.g., paved vs. unpaved, with or without rumble strips), density of roadside hazards, traveled path, or even encroached angle. The readers are referred to Daily et al. (5) and Mak and Bligh (8) for more discussion. The derived probability distribution of the lateral extent of encroachments from the proposed method can serve as a basis to obtain more elaborated distributions under different roadside conditions.

DISCUSSIONS

The illustration above shows that the method described in this paper can be a viable approach to estimating some of the basic encroachment parameters without actually collecting the data to estimate them, which can be very costly. Most importantly, it is straightforward to use such an approach to estimating basic encroachment parameters for various mainline traffic and design conditions, e.g., AADT, lane width, horizontal curvature, and vertical grade. The only premise is that a sound accident prediction model be developed. The better the accident prediction model, the better the estimate of basic roadside encroachment parameters can be expected.

In theory, the proposed method can be used for road sections of roadway classes other than the two-lane undivided roads illustrated in this paper. It is, however, not clear whether the extension of the proposed method to consider RORA at intersections is straightforward.

More research to explore the interrelationship between the accident-based approach and encroachment-based approach can help develop viable and cost-effective ways of quantifying roadside safety. The illustration provided in this paper is an example.

REFERENCES

- (1) Transportation Research Board. *Designing Safer Roads^{3/4}Practices for Resurfacing, Restoration, and Rehabilitation*. Special Report 214, TRB, National Research Council, Washington, D.C., 1987.
- (2) National Highway Traffic Safety Administration (NHTSA), *Traffic Safety Facts 1992*, Revised, March 1994.
- (3) Viner, J.G. Harmful Events in Crashes. *Accident Analysis & Prevention*. 25(2): 139-15; 1993.
- (4) Ray, M.H., J.F. Carney III, and K.S. Opiela, Emerging Roadside Safety Issues, *TR News* 177, March-April, 1995.
- (5) Daily, K.; W. Hughes, and H. McGee. *Experimental Plans for Accident Studies of Highway Design Elements: Encroachment Accident Study*. Prepared for FHWA; April 1994.
- (6) Mak, K.K. and D.L. Sicking. *Development of Roadside Safety Data Collection Plan*, Technical Report, Texas Transportation Institute, Texas A&M University System, College Station, Texas; 1992.
- (7) Viner, J.G. Rollovers on Sideslopes and Ditches. *Accident Analysis & Prevention*. 27(4): 483-491; 1995.
- (8) Mak, K.K. and R.P. Bligh, *Recovery-Area Distance Relationships for Highway Roadsides*, Phase I Report, NCHRP Project G17-11, Jan. 1996.
- (9) Zegeer, C.V., J. Hummer, D. Reinfurt, L. Herf, and W. Hunter. *Safety Effects of Cross-Section Design for Two-Lane Roads*. Volumes I and II. Chapel Hill: University of North Carolina; 1987.
- (10) Zegeer, C.V., R. Stewart, D. Reinfurt, F. Council, T. Neuman, E. Hamilton, T. Miller, and W. Hunter. *Cost-Effective Geometric Improvements for Safety Upgrading of Horizontal Curves*. Volumes I. Final Report. Chapel Hill: University of North Carolina; 1990.
- (11) Maycock, G. and R.D. Hall. *Accidents at 4-arm Roundabouts*. Transport and Road Research Laboratory Report 1120; 1984.
- (12) Miaou, S.-P. and H. Lum. Modeling Vehicle Accidents and Highway Geometric Design Relationships. *Accident Analysis and Prevention* 25(6):689-709; 1993.
- (13) Miaou, S.-P. The Relationship Between Truck Accidents and Geometric Design of Road Sections: Poisson Versus Negative Binomial Regressions. *Accident Analysis & Prevention* 26(4): 471-482; 1994.
- (14) Miaou, S.-P., P.S. Hu, T. Wright, S.C. Davis, and A.K. Rathi. *Development of Relationship Between Truck Accidents and Geometric Design: Phase I*. Publication No. FHWA-RD-91-124, FHWA, U.S. Department of Transportation, 1993.
- (15) Miaou, S.-P. *Measuring the Goodness-of-Fit of Accident Prediction Models*. FHWA-RD-96-040, FHWA, U.S. Department of Transportation, December 1996, 121pp.

- (16) Glennon, J.C. *Roadside Safety Improvement Programs for Freeways*^{3/4}*A Cost Effectiveness Priority Approach*. NCHRP Report 148, TRB, National Research Council, Washington, D.C., 1974.
- (17) Rodgman, E., C. Zegeer, and J. Hummer. *Safety Effects of Cross-Section Design for Two-Lane Roads - Data Base User's Guide*, report submitted to FHWA, Revised, Nov. 1989.
- (18) Miaou, S.-P., and H. Lum. Statistical Evaluation of the Effects of Highway Geometric Design on Truck Accident Involvements. In *Transportation Research Record 1407*, TRB, National Research Council, Washington, D.C., 1993, pp. 11-23.
- (19) Hutchinson, J.W. and T.W. Kennedy. *Medians of Divided Highways*^{3/4}*Frequency and Nature of Vehicle Encroachments*. Engineering Experiment Station Bulletin 487, University of Illinois, June 1966.
- (20) Cooper, P. *Analysis of Roadside Encroachments*^{3/4}*Single Vehicle Run-Off-Road Accident Data Analysis for Five Provinces*. B.C. Research, Vancouver, Canada, March 1980.

LIST OF TABLES

Table 1. Estimated regression coefficients of a negative binomial regression model and associated statistics for single-vehicle run-off-the-road accidents23

LIST OF FIGURES

Figure 1. Illustration of single-vehicle run-off-the-road accident rates for various lane widths and sideslopes24

Figure 2. Single-vehicle run-off-the-road accident rates for a given sideslope versus single-vehicle run-off-the-road accident rate for a sideslope of 7:125

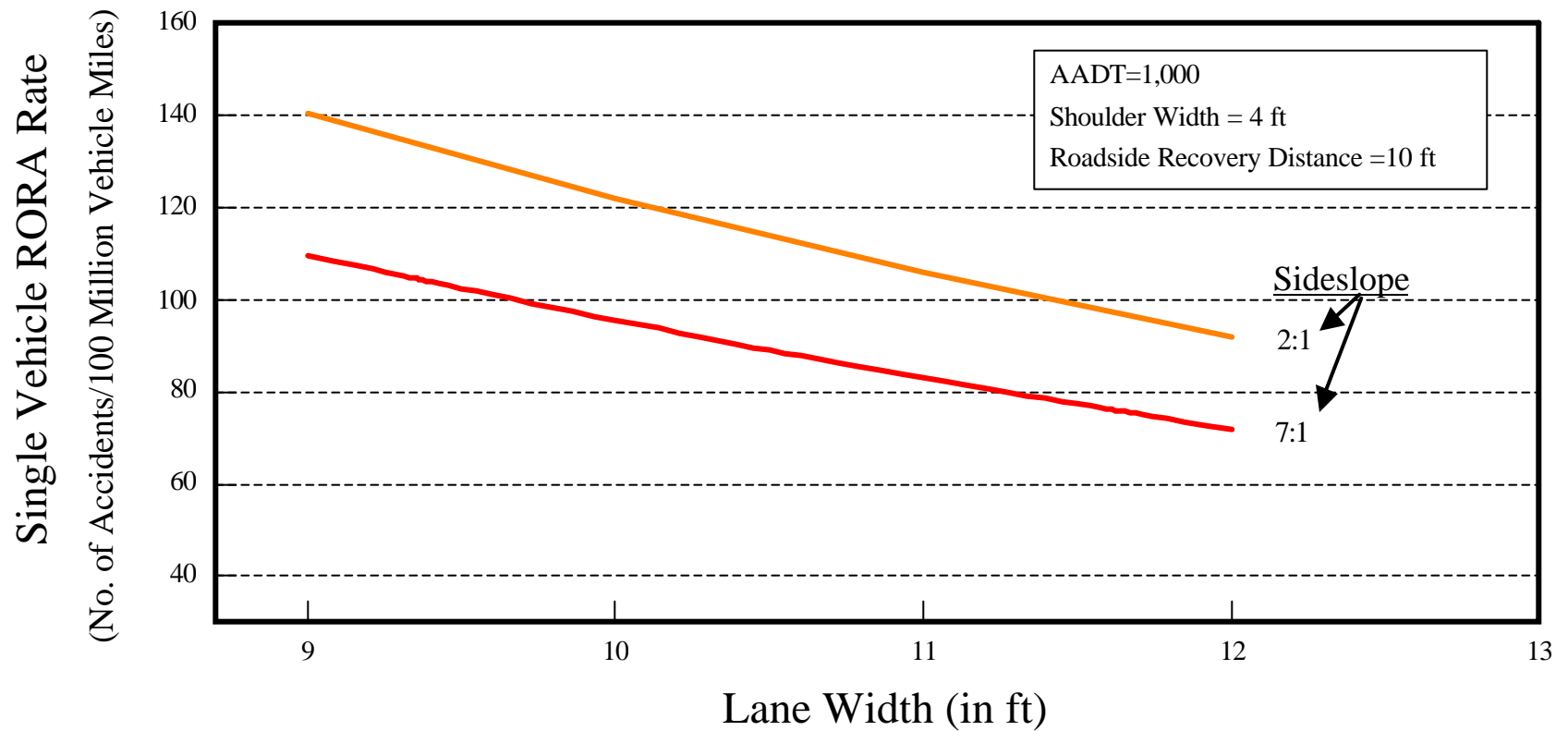
Figure 3. Comparison of the derived roadside encroachment frequency from the accident prediction model shown in Table 1 and observed frequencies from earlier studies26

Figure 4. Comparison of various probability distributions of the lateral extent of encroachments.....27

Table 1. Estimated regression coefficients of a negative binomial regression model and associated statistics for single-vehicle run-off-the-road accidents.

Covariate and Parameter	Estimated Parameter Value
β_1 Dummy intercept (=1)	1.20043 ("0.46;2.62)
β_2 Dummy variable for Michigan (1=Michigan; 0=otherwise)	0.6076 ("0.12;4.92)
β_3 Dummy variable for Washington (1=Washington; 0=otherwise)	0.4218 ("0.13;3.16)
β_4 AADT per lane (in 10^3)	-0.1783 ("0.04;-4.57)
β_5 Lane width (in ft)	-0.1411 ("0.04;-3.43)
β_6 Median clear roadside recovery distance (in ft)	-0.01375 ("0.007;-1.97)
β_7 Paved shoulder width (in ft)	-0.0881 ("0.014;-6.38)
β_8 Earth, grass, gravel, or stabilized shoulder width (in ft)	
β_9 Median sideslope (e.g., 3:1 and 7:1 slopes are recorded as $1/3=0.33$ & $1/7=0.14$, respectively.)	0.6920 ("0.45;1.54)
β_{10} Terrain type (0=flat; 1=mountainous+rolling)	0.2939 ("0.09;3.35)
β_{11} Posted speed limit (in mi/h)	-----
β_{12} Number of intersections per mile	-----
β_{13} Number of driveways per mile	0.0129 ("0.006;2.33)
β_{14} Number of bridges per mile	0.2016 ("0.095;2.13)
Dispersion parameter of the NB model (α)	0.3988 ("0.036;11.0)
$L(\alpha, \beta)$ (=loglikelihood function)	-1646.8
Akaike Information Criterion Value	3317.5
Expected vs. observed total number of accidents	4,709 vs 4,632

Notes: (1) 596 rural two-lane undivided road sections; total length=1,788 mi; about 5 years of accident data (1980-1984).
(2) Values in parentheses are asymptotic standard deviation and t-statistics of the coefficients above.
(3) ----- indicates "not included in the model."
(4) 1 mile = 1.61 km, 1 ft = 0.3048 m.



(1 mi = 1.61 km; 1 ft = 0.3048 m)

Figure 1. Illustration of single-vehicle run-off-the-road accident rates for various lane widths and sideslopes.

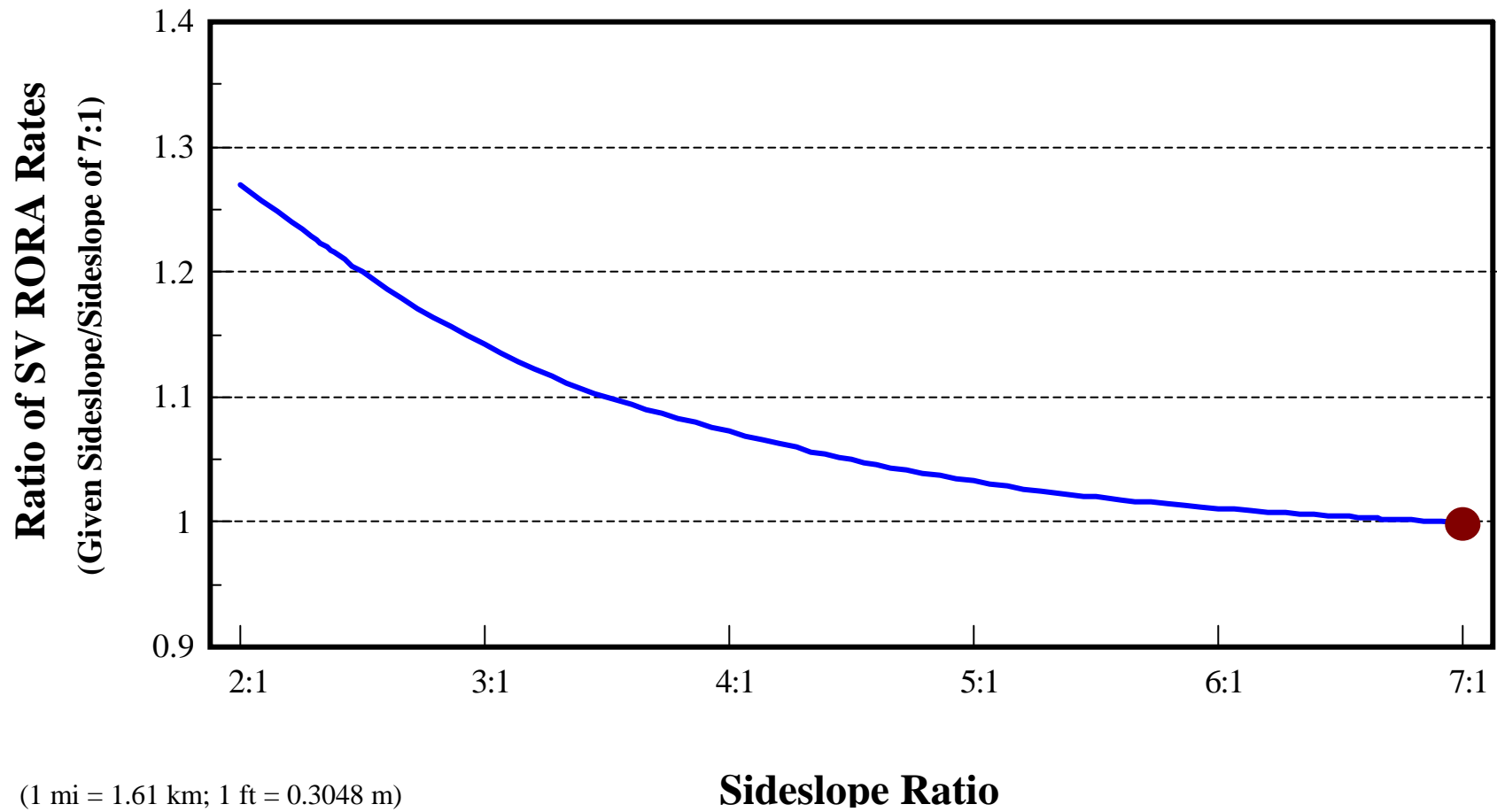


Figure 2. Single-vehicle run-off-the-road accident rates for a given sideslope versus single-vehicle run-off-the-road accident rate for a sideslope of 7:1

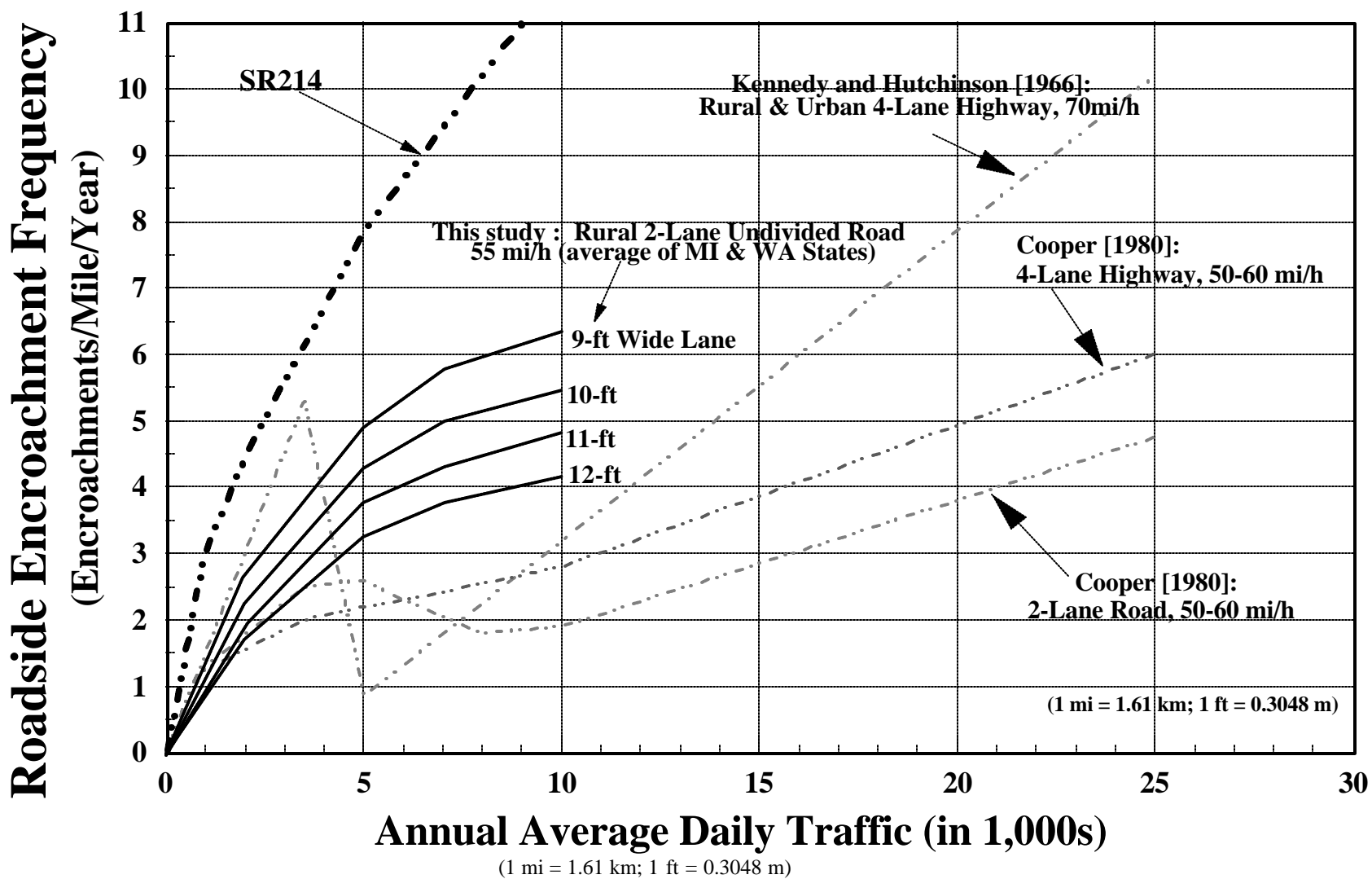


Figure 3. Comparison of the derived roadside encroachment frequency from the accident prediction model shown in Table 1 and observed frequencies from earlier studies.

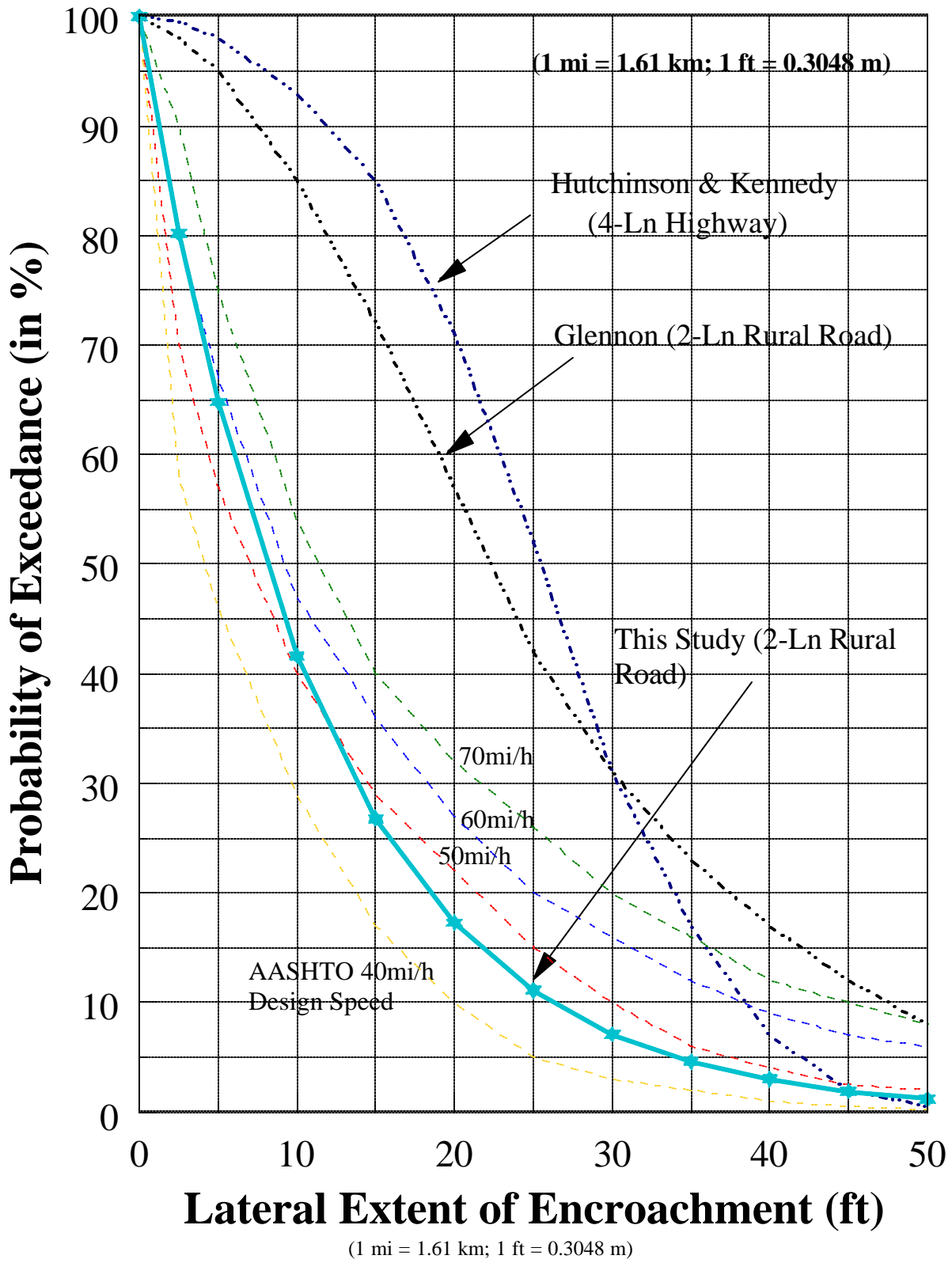


Figure 4. Comparison of various probability distributions of the lateral extent of encroachments.

APPENDIX B

Working Paper

ANOTHER LOOK AT THE RELATIONSHIP BETWEEN ACCIDENT- AND ENCROACHMENT-BASED APPROACHES TO RUN-OFF-THE-ROAD ACCIDENTS MODELING

Shaw-Pin Miaou

Research Staff Member

Center for Transportation Analysis, Energy Division

Oak Ridge National Laboratory

P.O. Box 2008, MS 6073, Building 3156, Oak Ridge, TN 37831, USA

Phone: (423) 574-6933; Fax: (423) 574-3851; E-Mail: PNI@ORNL.GOV

August 1997, Revised January 1998

ABSTRACT

Understanding the relationships between roadside accidents and roadside design is imperative to developing cost-effective, road-related countermeasures to improve roadside safety. Much of what is known today about the relationships remains to be qualitative in nature. Recent studies have suggested that new, cost-effective analysis approaches and data collection efforts are essential if a more quantitative basis of such relationships is to be developed. Historically, models used in previous studies to develop the relationships have been categorized as using either an accident-based approach or an encroachment-based approach. The former has a solid statistical ground, but has been criticized as being overly empirical and lacking engineering basis. The latter, on the other hand, has analytical and engineering strengths, but has been described as being full of subjective assumptions and lack of sufficient supporting data. In addition, these two approaches seem to have been treated as two competing, disconnected approaches, and very few attempts have been made by roadside safety researchers to combine the strengths of both. The purpose of this study was to look for ways to combine the strengths of both approaches. The specific objectives were (1) to present the encroachment-based approach in a more systematic and coherent way so that its limitations and strengths can be better understood from both the statistical and engineering

standpoints, and (2) to apply the analytical and engineering strengths of the encroachment-based approach to the formulation of mean functions in accident-based models.

To demonstrate the strength of mean functions so obtained, accident-based models were developed using such mean functions for guardrail and utility pole accidents. Furthermore, to show how the accident-based model can be useful to the encroachment-based model, the developed accident models were used to estimate the roadside encroachment rate—a basic input parameter that is required by the encroachment-based model and is expensive and technically difficult to collect. The estimated rates were found to be consistent with those obtained in earlier encroachment-based studies. This is an indication that estimating basic encroachment parameters using accident-based models can be a viable approach to reducing encroachment data collection cost. In addition, unlike estimating encroachment parameters from the field-collected encroachment data, the use of accident-based models to estimate encroachment parameters does not require the development of a procedure to distinguish between controlled and uncontrolled encroachments, which can be subjective and technically difficult to do in practice. This paper concludes with a discussion on future research.

Key Words: *Run-Off-the-Road Accident, Roadside Design, Vehicle Roadside Encroachment, Encroachment-Based Model, Accident-Based Model*

ANOTHER LOOK AT THE RELATIONSHIP BETWEEN ACCIDENT- AND ENCROACHMENT-BASED APPROACHES TO RUN-OFF-THE- ROAD ACCIDENTS MODELING

INTRODUCTION

Understanding the relationships between roadside accidents and roadside design is imperative to developing cost-effective, road-related countermeasures to improve roadside safety. To date, much of what is known about the relationships remains to be qualitative in nature or dependent on subjective engineering guesses [Ray et al., 1995; Daily et al., 1997]. Recent studies suggested that new and cost-effective analysis approaches and data collection efforts are essential if a more quantitative basis of such relationships is to be developed [Mak and Sicking, 1992; Viner, 1995; Mak and Bligh, 1996]. Models used in previous studies to develop the relationships between run-off-the-road accidents (RORA) and roadside hazards, such as utility poles, trees, guardrail, median barriers, and embankments, have been categorized as using either an accident-based approach or an encroachment-based approach [Transportation Research Board (TRB), 1987; Daily et al., 1997].

The accident-based approach uses statistical regression models to develop the relationships in which the RORA frequency of hitting a particular or a combination of roadside hazards is the dependent variable, and traffic flows, roadway mainline designs, roadside designs, and other variables are the explanatory variables (or covariates) [Zegeer et al., 1987; Zegeer et al., 1990; Miaou, 1996]. In the last decade or so, there has been a steady realization of the statistical advantages of using the Poisson and negative binomial (NB) regression models over the conventional normal distribution-based regression models when this approach is used to model road accidents [Maycock and Hall, 1984; Miaou and Lum, 1993]. The theory behind the Poisson and NB regression accident-based models has been discussed quite extensively in many recent publications [e.g., Miaou, 1994; Maher and Summersgill, 1996; Miaou, 1996]. The goal of these accident-based models is not only to estimate the expected number of accidents and its association with key covariates, but also to estimate the statistical uncertainty associated with the estimates. In general, these accident-based models have been developed with a solid statistical ground.

Under the Poisson and NB regression models, a mean function, which is a function that relates the mean (or expected) number of accidents to the covariates, is typically assumed to have an exponential form. This functional form has several desirable mathematical properties and has been widely accepted in other research areas, such as biostatistics and econometrics [Miaou, 1996]. Some of the desirable properties include: (1) it is a multiplicative function that allows interactive effects of covariates on accidents to be easily represented; (2) it ensures that the mean accident rate is always nonnegative; and (3) it is mathematically convenient to obtain standard statistical inferences for the model. However, the use of such a functional form has been criticized as being overly empirical and lacking engineering basis.

The encroachment-based approach uses a series of conditional probabilities to describe the sequence of events resulting in a roadside accident [Glennon, 1974; TRB, 1987; Daily et al., 1997]. A typical sequence of events considered by this approach is: (1) an errant vehicle leaves the traveled way and encroaches on the shoulder; (2) the location of encroachment is such that the path of travel is directed towards a potentially hazardous roadside object; (3) the hazardous object is sufficiently close to the travel lanes that control is not regained before encounter or collision between vehicle and object; and (4) the collision is sufficiently severe enough to result in an accident of some level of severity. The idea of the encroachment-based approach was to formulate and estimate these conditional probabilities based on a combination of traffic, vehicle dynamics, and driver behavior theories. Appendix F of Transportation Research Board (TRB) Special Report 214 (SR214) provides a good description of the concept behind the encroachment-based approach and its application on two-lane undivided roads [TRB, 1987].

Over the last 30 years, there has been a constant effort to develop and refine the encroachment-based models. Despite these efforts, the encroachment-based approach is still being criticized as being full of subjective assumptions and lacking sufficient supporting data [Daily et al., 1997]. In addition, available vehicle encroachment data, including encroachment rates, were collected on a small number of road sections and are largely outdated. The Federal Highway Administration (FHWA) and TRB have been addressing the requirements and collection of such data through their sponsorship of several roadside safety projects. As a result, rather comprehensive data collection plans have been proposed, and results of pilot data collection efforts have been reported [Mak and Sicking, 1992; Mak and Bligh, 1996; Daily et al., 1997]. A review of these

plans and pilot data collection results suggests that the cost of collecting the required roadside field data will be very high. Furthermore, the validity of any field-collected encroachment data may be questionable because of the technical difficulty in distinguishing between controlled (or intentional) and uncontrolled (or unintentional) encroachments.

A recent review of the encroachment-based approach and its relationship to the accident-based approach is given in Miaou [1996]. The encroachment-based approach is appealing because of its analytical and engineering strengths. It allows useful results from other studies, especially those in the areas of driving behavior and vehicle dynamics, to be directly incorporated into the model in a sensible way. In addition, systematic exploration and assessment of different road- and vehicle-based countermeasures, which have the potential of reducing the probability of the occurrence of each encroachment event described above, can be conducted with such an approach. The study by Fancher et al. [1994] is an example of using the encroachment-based approach to assess the potential benefits of using Intelligent Transportation Systems (ITS) technologies to improve road safety.

Historically, researchers on roadside safety seem to have treated these two approaches as two competing, disconnected approaches and seldom or never attempt to seek the opportunity to combine the strengths of both [Mak and Sicking, 1992; Miaou, 1996]. In a recent study, Miaou attempted to point out the complementary nature of the two approaches and suggested that the accident-based approach can benefit from the encroachment-based thinking in obtaining a mean function that has better engineering basis and interpretation [Miaou, 1996; Miaou, forthcoming]. Furthermore, because the data required to estimate basic encroachment parameters, such as encroachment rates, for use in the encroachment-based model are expensive and difficult to collect in practice, Miaou proposed a method to estimate some basic encroachment parameters using accident-based models. The method was developed based on an exploration of the probabilistic relationship between a roadside encroachment event and an RORA event. Miaou illustrated the concept and use of such a method by first using data from three States, which were contained in an FHWA Seven States Cross-Section Data Base [Rodgman et al., 1989], to develop a RORA prediction model for rural two-lane undivided roads. The model was then used to estimate encroachment rates by setting the clear zone width to zero and the sideslope ratio to 1:1 in the RORA prediction model.

The study presented in this paper is an extension of Miaou's study [Miaou, 1996; Miaou, forthcoming]. The purpose of this study was to look for ways to combine the strengths of both approaches in roadside safety research. The specific objectives were (1) to present the encroachment-based approach in a more systematic and coherent way so that its limitations and strengths can be better understood from both statistical and engineering standpoints, and (2) to apply the analytical and engineering strengths of the encroachment-based thinking to the formulation of mean functions in accident-based models. To demonstrate the use of mean functions so obtained, an accident-based model was developed using such mean functions for guardrail and utility pole accidents from the same data base as that used by Miaou [1996]. Furthermore, to show how the accident-based model can be useful to the encroachment-based model, similar to the approach proposed by Miaou, encroachment rates are estimated using the developed guardrail and utility pole accident models. The rates were compared with those estimated by Miaou [1996] and other encroachment-based studies, such as Hutchinson and Kennedy [1966], Cooper [1980], and SR214 [1987].

This paper is organized as follows: Section 2 provides a systematic examination of the encroachment-based thinking, addressing its limitations and strengths from both the statistical and engineering standpoints. Section 3 describes a way to formulate mean functions for accident-based models using encroachment-based thinking described in Section 2. Section 4 uses the formulation suggested in Section 3 to develop accident-based prediction models for guardrail and utility pole accidents and then estimates roadside encroachment rates from these models. This paper concludes with a discussion of future work.

The following discussion focuses on two-lane, undivided roads. However, the extension to other roadway types should be straightforward. Also, in the discussion, a "roadside encroachment" is said to occur when an errant vehicle crosses the outside edges of the travelway and encroaches on either the inside or outside shoulder. Thus, for a two-lane, undivided road that has no inside shoulder, the total number of roadside encroachments includes departures of vehicles from near-side and far-side edges of the travelway in both directions. It is also important to note that roadside encroachments refer only to uncontrolled (or unintentional) encroachments. In other words, the "controlled or intentional encroachments" resulting from vehicles intentionally driven

outside of the travel lane (e.g., onto shoulders and traversable medians) are not counted as encroachments.

ENCROACHMENT-BASED THINKING

Consider a vehicle traveling through a road section of length L . The road section is characterized by its mainline and roadside conditions. On the mainline, the condition is characterized by its key design attributes, including lane width, horizontal curvature, and vertical grade, and by its traffic conditions, such as traffic density and car-truck mix percentages. On the roadside, the number and combination of various types and sizes of roadside objects, their locations along the road section, and their lateral offsets from the edge of travelway are some of the main safety-related characteristics of interest.

For clarity, in the following presentation, it may be necessary in some instances to indicate which road section within the sample sections is being considered. Under such instances, we will assume, without loss of generality, that the i th sample road section is under consideration.

Overall Concept

For a particular type of roadside object, such as guardrails or utility poles (made of the same material), the passage that leads the subject vehicle to hit one of these objects and results in a reportable accident is modeled as four sequential stochastic processes. Each of the four processes is modeled by a conditional probability. Figure 1 gives an overview of these processes and the key determinants that affect the outcome of each process. Process 1 determines the probability that the vehicle will encroach on the roadside. If the vehicle encroaches, the encroachment is characterized by its encroachment speed and angle, which are used as input to Process 2. Given an encroachment speed and angle, Process 2 determines the probability that the encroachment location of the vehicle is in a potentially hazardous envelope associated with one of the roadside objects under consideration, which makes the impact with the object possible. If the encroaching vehicle is in a hazard envelope, Process 3 determines whether the vehicle will encroach far enough to collide with the object. The key output of Process 3 is an impact speed, which can be zero (i.e., no collision). Provided that the vehicle collides with the object, the impact speed is used as input to Process 4 to determine whether the impact will result in a reportable accident.

For ease of exposition, this paper uses the following notations: \mathbf{x} symbolizes the occurrence of a vehicle roadside encroachment; H_q , C_q , and A_q represent, respectively, the hazard envelope, collision event, and accident event that are associated with the q th roadside object on the road section, where $q = 1, 2, \dots, Q$, and Q is the total number of objects on both sides of the road section; $X^{(1)}$, $X^{(2)}$, $X^{(3)}$, and $X^{(4)}$ denote key determinants associated with Processes 1, 2, 3, and 4, respectively, that are observable and available; and $Z^{(1)}$ represents those unobservable and unavailable variables associated with Process 1. As noted from the accident-based literature, variables in $Z^{(1)}$ are mainly driver- and vehicle-related variables that are usually unavailable by individual site [Miaou, 1996]. Using these notations, the conditional probabilities associated with these four processes, which pertain to the q th object on the road section, are further denoted by $P(\mathbf{x}|X^{(1)}, Z^{(1)})$, $P(\text{In } H_q | \mathbf{x}, X^{(2)})$, $P(C_q | \text{In } H_q, X^{(3)})$, and $P(A_q | C_q, X^{(4)})$. Note that (1) “ $\text{In } H_q$ ” symbolizes that the vehicle is in the hazard envelope and implies that a roadside encroachment has occurred; (2) for the models to be discussed later in this paper on $P(C_q | \text{In } H_q, X^{(3)})$, collision C_q implies that the encroachment is in hazard envelope H_q ; and (3) accident A_q implies the occurrence of collision C_q .

Mathematically, the encroachment-based approach separates the probability of a vehicle being involved in A_q , given determinants $X^{(1)}$, $X^{(2)}$, $X^{(3)}$, $X^{(4)}$, and $Z^{(1)}$, into a series of conditional probabilities as follows:

$$\begin{aligned}
& P(A_q | X^{(1)}, X^{(2)}, X^{(3)}, X^{(4)}, Z^{(1)}) \\
&= P(\mathbf{x} | X^{(1)}, Z^{(1)}) P(A_q | \mathbf{x}, X^{(2)}, X^{(3)}, X^{(4)}) \\
&= P(\mathbf{x} | X^{(1)}, Z^{(1)}) P(\text{In } H_q | \mathbf{x}, X^{(2)}) P(C_q | \text{In } H_q, X^{(3)}) P(A_q | C_q, X^{(4)})
\end{aligned} \tag{1}$$

At the microscopic level, the mechanics and driver behavior that determine the outcome of each of the four processes can be quite complex. To make the concept workable and useable, there has been a conscientious effort attempting to simplify each of these processes based on engineering judgment and limited, available data. How each process has been and can potentially be treated in the encroachment-based study is described in more detail in the rest of the section.

Process 1

One of the efforts made to simplify the analytical procedure is to separate Process 1 from the rest of the processes. This is done by introducing the assumption that roadside design has a negligible effect on roadside encroachment probability. In other words, this assumption says that the probability of encroachments can be solely determined from mainline conditions. This assumption simplifies the analytical procedure significantly. Specifically, it allows the analysts to stay focused on the analysis of the last three processes, which pertain to the effect of alternative roadside designs on the accident probability, without worrying about the roadside encroachment rates and characteristics being altered as a result of different roadside designs. However, the validity of this assumption has not been formally challenged and may be debatable. For example, some may believe that some roadside conditions, such as a sharp sideslope, can significantly affect a driver's driving behavior (e.g., driver's attentiveness) and therefore affect roadside encroachment rates.

Using this assumption, previous encroachment-based studies typically started the analysis with the premise that data on encroachment rates and two key encroachment characteristics, namely, encroachment speed and angle, are available either from some data collection efforts or can be pre-estimated. Encroachment rates, angles, and speeds are, however, expected to vary by weather condition, roadway functional class, average annual daily traffic (AADT), lane width, horizontal curvature, vertical grade, and even car-truck mix percentage [Mak and Sicking, 1992]. Thus, besides the potential technical difficulties to be discussed next, the effort required to collect a comprehensive set of encroachment data under all these conditions will be tremendous.

Many data collection instruments have been used to obtain roadside encroachment data, including observing tire-tracks, monitoring maintenance records of roadside objects, and using electronic monitoring equipment such as video cameras [Mak and Sicking, 1992; Daily et al., 1997]. However, so far, most of the data collection efforts have been small-scale and experimental in nature and were not considered successful. As indicated earlier, even if the controlled encroachments can be distinguished from the uncontrolled encroachments, the effort required to collect all of the necessary data is expected to be expensive. One additional note regarding controlled and uncontrolled encroachments is that no formal, quantitative definitions of them exist. Recognizing that oftentimes there is a fine line between a controlled and an

uncontrolled encroachment, the procedure used to remove controlled encroachments from the collected encroachment data are bound to be subjective.

Note that, for simplicity, the discussion in this paper does not distinguish far-side and near-side (i.e., left- and right-side) encroachments. When accidents are available by side of road and direction of travel and when roadside objects, and perhaps traffic, are inventoried by side of road, there may be some incentive to consider them separately, which is conceptually not difficult to do.

Output of Process 1

The output of Process 1 is the occurrence or non-occurrence of an encroachment event. The probability of the occurrence of the event is represented by a conditional probability

$P(x|X^{(1)}, Z^{(1)})$. If an encroachment occurs, the encroachment is further characterized by its encroachment angle and speed, two key parameters which will be used in the subsequent processes to determine whether the encroachment can result in a collision with a roadside object. As indicated before, the assumption is that these basic encroachment parameters, including the encroachment probability, $P(x|X^{(1)}, Z^{(1)})$, and encroachment speed and angle, are not affected by roadside conditions.

Input to Processes 2-4

The input to Processes 2-4 is an encroachment event that is characterized by its speed and angle. The speed and angle are treated as random variables generated from a joint probability density function, $f(v, f)$, where v and f represent encroachment speed and angle, respectively. The conditional probability for Processes 2-4 can now be re-expressed in terms of v and f as

$$\begin{aligned}
 & P(A_q | \mathbf{x}, X^{(2)}, X^{(3)}, X^{(4)}) \\
 &= \int_f \int_v P(A_q | \mathbf{x}, v, \mathbf{f}, X^{(2)}, X^{(3)}, X^{(4)}) f(v, \mathbf{f}) dv d\mathbf{f} \\
 &= \int_f \int_v P(InH_q | \mathbf{x}, v, \mathbf{f}, X^{(2)}) P(C_q | InH_q, v, \mathbf{f}, X^{(3)}) P(A_q | C_q, v, \mathbf{f}, X^{(4)}) f(v, \mathbf{f}) dv d\mathbf{f}
 \end{aligned} \tag{2}$$

Given $f(v, \theta)$, the focus of the encroachment-based studies has been on the three conditional probabilities: $P(\text{In } H_q | x, v, f, X^{(2)})$, $P(C_q | \text{In } H_q, v, f, X^{(3)})$, and $P(A_q | C_q, v, f, X^{(4)})$.

Due to lack of data on encroachment speed and angle, the density functions that have been used in the literature and current roadside analysis software are largely chosen using engineering judgment [Mak and Sicking, 1992; Daily et al., 1997]. To facilitate the following discussion, Figure 2 gives an example joint probability density of encroachment speed and angle. Without real data, this example density function is considered to be as plausible and complex as any function that has been used or proposed in the encroachment-based studies by TRB [1987], Mak and Sicking [1992], Daily et al. [1997].

In Figure 2, the encroachment speed density is first represented by a triangular function as

$$\begin{aligned}
 f(v) &= \frac{2(v - v_{\min})}{(v_{\text{ref}} - v_{\min})(v_{\max} - v_{\min})}, \text{ if } v_{\min} \leq v \leq v_{\text{ref}} \\
 &= \frac{2(v_{\max} - v)}{(v_{\max} - v_{\min})(v_{\max} - v_{\text{ref}})}, \text{ if } v_{\text{ref}} < v \leq v_{\max} \\
 &= 0, \text{ otherwise}
 \end{aligned} \tag{3}$$

where v_{ref} is a reference speed that relates to the posted speed limit and design speed, and v_{\min} and v_{\max} are the minimum and maximum encroachment speeds, respectively. Second, the maximum possible encroachment angles, f_{\max} , is postulated to be dependent of the encroachment speed, v , in a linear fashion as follows:

$$f_{\max}(v) = f_{\max}(v_{\min}) - \left[\frac{f_{\max}(v_{\min}) - f_{\max}(v_{\max})}{v_{\max} - v_{\min}} \right] (v - v_{\min}) \text{ for } v_{\min} \leq v \leq v_{\max} \tag{4}$$

where $f_{\max}(v_{\min})$ and $f_{\max}(v_{\max})$ are, respectively, the maximum possible encroachment angles when encroaching at speeds of v_{\min} and v_{\max} . That is, as the encroachment speed increases, the

possible encroachment angle decreases in a linear fashion. This relationship is based on the notion that most vehicles do not rollover at the time of encroachment. That is, the roadholding capacity that a vehicle can provide is not exceeded at the outset of most of the encroachments. Third, the probability density of the encroachment angle f , given f_{\max} , is represented by another triangular function as

$$f(\mathbf{f} | \mathbf{f}_{\max}) = \frac{2}{\mathbf{f}_{\max} - \mathbf{f}_{\min}} \left[1 - \frac{\mathbf{f} - \mathbf{f}_{\min}}{\mathbf{f}_{\max} - \mathbf{f}_{\min}} \right], \text{ if } \mathbf{f}_{\min} \leq \mathbf{f} \leq \mathbf{f}_{\max}$$

$$= 0$$
(5)

Note that, mathematically, it is straightforward to combine all three equations into a joint density function by using the relationship

$$f(\mathbf{v}, \mathbf{f}) = f(\mathbf{f} | \mathbf{v}) f(\mathbf{v})$$

$$= f(\mathbf{f} | \mathbf{f}_{\max}) f(\mathbf{v})$$
(6)

However, this mathematical expression is quite complicated and will not be presented here. An obvious deficiency of this joint density function is that it ignores the effect of horizontal curvatures on f .

To have some understanding of the statistical properties of the exemplified joint density function, a Monte-Carlo simulation was performed with the following parameter values: $\mathbf{v}_{\min}=0$, $\mathbf{v}_{ref}=55$ mi/hr, $\mathbf{v}_{\max}=70$ mi/hr, $f_{\max}(\mathbf{v}_{\min})=40^\circ$, $f_{\max}(\mathbf{v}_{\max})=15^\circ$, and $f_{\min}=0.25^\circ$. The reason why $f_{\min}=0.25^\circ$ is used, instead of 0° , will be given later. The simulation results show that the expected value of encroachment speed, expressed as $E[\mathbf{v}]$, is 41.7 mi/hr, and the unconditional expectations $E[f]$ and $E[f_{\max}]$ are, respectively, equal to 8.5° and 25.1° . Note that the same set of parameter values for the joint density function, $f(\mathbf{v}, \mathbf{f})$, was used for all of the Monte-Carlo simulations performed in this study.

Process 2

Process 2 determines $P(\text{In } H_q | \mathbf{x}, \nu, \mathbf{f}, X^{(2)})$ for each of the Q objects. Figure 3 shows a commonly used formula to compute the size of the hazard envelope, given f , vehicle swath width (W_{veh}), and length and width of the considered object ($\ell_{obj,q}$ and $W_{obj,q}$). This is expressed as

$$\ell_{env,q} = \ell_{obj,q} + W_{obj,q} \cot(\mathbf{f}) + W_{veh} \csc(\mathbf{f}) \quad (7)$$

This formula has been widely used and discussed [TRB, 1987; Daily et al., 1997]. It is based on the assumption that the road section is a straight section with no horizontal curvature and that the trajectory of the encroaching vehicle is a straight line.

Hazard envelopes can, of course, overlap when multiple objects exist and are located closely to one another. This is especially true when f is small. By considering the potential for overlapping of H_q , the conditional probability can be expressed as

$$\begin{aligned} P(\text{In } H_q | \mathbf{x}, \nu, \mathbf{f}, X^{(2)}) &= P(\text{In } H_q | \mathbf{x}, \mathbf{f}, X^{(2)}) = \frac{\ell_{env,q} - OL_q(\mathbf{f})}{2L} \\ &= \frac{\ell_{obj,q} + W_{obj,q} \cot(\mathbf{f}) + W_{veh} \csc(\mathbf{f}) - OL_q(\mathbf{f})}{2L} \quad (8) \end{aligned}$$

where L is the length of the road section, and $OL_q(\mathbf{f})$ represents an adjustment of the size of H_q that is overlapped by other objects and is a function of f . The use of $2L$ in the denominator requires the assumption that encroachments are equally likely to occur on the right and left sides of the road, and that the encroachment is equally likely to occur at any location within the road section. These assumptions are good only for a straight and level road section that is homogeneous in traffic and design variables, such as AADT and lane width, within the road section.

Estimating the size of overlapping envelopes can be a tedious bookkeeping process and is usually avoided in the modeling stage by either selecting objects that are typically far away from one another or by treating closely located objects as one continuous object [TRB, 1987; Daily et al., 1997; Rodgman et al., 1989]. Another potential problem with estimating the H_q , which is usually ignored, is that the envelope of those objects that are located close to the end points of the road section can have significant part of the envelope falling on adjacent sections. Of course, adjacent sections may have envelopes falling on the section under consideration. If the objects are evenly located across the section, this “boundary problem” will roughly cancel out. Otherwise, more tedious bookkeeping procedures may be required.

In practice, when a type of point object is considered, $\ell_{obj,q}$ and $W_{obj,q}$ are usually set to constants for all Q objects. In addition, when a round-shaped object is considered, it is typically treated as a squared object and $\ell_{obj,q}$ and $W_{obj,q}$ are set approximately equal to the diameter of the object. For example, for utility poles, $\ell_{obj,q} = W_{obj,q} = 8$ inches have been used [TRB, 1987]. For a particular type of continuous object considered, such as guardrails, the length $\ell_{obj,q}$ varies over q , but $W_{obj,q}$ remains fairly constant for all objects. Also, W_{veh} is fixed and determined with a design vehicle (e.g., a mid-sized car) in mind. For example, W_{veh} was set to 6 ft in SR214 and to 12 ft in *Roadside Design Guide* [American Association of State Highway and Transportation Officials (AASHTO), 1989]. Note that, for the point object, the size of the hazard envelope, as calculated in Eq. (7), is dominated by the term $W_{veh} \csc(f)$ because W_{veh} is considerably larger than $\ell_{obj,q}$ and $W_{obj,q}$. On the other hand, for the continuous object, $\ell_{obj,q}$ is usually the dominant term in Eq. (7).

To gain some understanding of the size of H_q , two Monte-Carlo simulations were conducted with the same joint density $f(v,f)$ as in the previous simulation and with W_{veh} set to 9 ft. The first simulation is intended to represent the size of H_q for a long guardrail with $\ell_{obj,q} = 1,320$ ft (or 0.25 mi) and $W_{obj,q} = 1$ ft. The simulation results show that the minimum, average, and maximum sizes of the envelopes are about 1,336 ft, 1,493 ft, and 3,610 ft, respectively. (Note that the average size of the envelope is a simulation-based estimate of the integral

$\dot{\mathbf{Q}}_f \dot{\mathbf{Q}}_v \left[\ell_{obj,q} + W_{obj,q} \cot(f) + W_{veh} \csc(f) \right] f(v, f) dv df$. In this simulation, on average, $W_{veh} \csc(f) + W_{obj} \cot(f) = 173$ ft, in which $W_{veh} \csc(f) = 156$ ft and $W_{obj} \cot(f) = 17$ ft. This suggests that, for a short continuous object, e.g., $\ell_{obj,q} < 500$ ft, the proportion of the envelope that is attributed to vehicle swath width and object width may not be ignored. This is mainly because f is typically small (for straight road sections), which makes $\csc(f)$ and $\cot(f)$ large.

The second simulation run was performed to represent the envelope of a utility pole that was assumed to have an 8-inch diameter. The corresponding minimum, average, and maximum sizes of the envelope are 16 ft, 168 ft, and 2,214 ft, respectively. In this simulation, on average, $W_{veh} \csc(f) = 156$ ft and $W_{obj} \cot(f) = 12$ ft. This suggests that, even with a relatively small point object like a utility pole, the size of the envelope can be very wide due, again, to vehicle swath width and object width, as a result of small encroachment angles. These two simulations indicate that $\ell_{obj}/2L$ will not be a good approximation of the conditional probability in Eq. (8) in practice when point objects are considered and may not be good for continuous objects when the length of the object is short.

Note that the average sizes of $W_{veh} \csc(f)$ and $W_{obj} \cot(f)$ obtained from this utility pole simulation is considerably larger than, for example, that obtained by Hutchinson and Kennedy [1966] and that used in *Roadside Design Guide* [AASHTO, 1989]. In Hutchinson and Kennedy, a near-side encroachment angle of 6.1° and a far-side encroachment angle of 11.5° were estimated from limited encroachment data. These angles were used to compute the average size of the envelope using Eq. (7). Assuming that two-thirds of the encroachments are near-side encroachments and one-third are far-side encroachments, this gives an average encroachment angle of about 8° . Now, using the same vehicle swath width of 9 ft as in the simulation, we have $W_{veh} \csc(f) + W_{obj} \cot(f) = 64.7$ ft + 4.7 ft = 69.4 ft. In *Roadside Design Guide*, an encroachment angle of 15.2° is recommended for both near-side and far-side encroachments. The basis of this recommendation is, however, not clear. Nevertheless, under this recommendation and using the same vehicle swath width, $W_{veh} \csc(f) + W_{obj} \cot(f) = 34.3$ ft + 2.5 ft = 36.8 ft. Thus, assuming that the vehicle swath width of 9 ft can be agreed on, the size of

$W_{veh} \csc(f) + W_{obj} \cot(f)$ obtained from the utility pole simulation in this study is, respectively, about 2.4 and 4.5 times that used by Hutchinson and Kennedy [1966] and *Roadside Design Guide* [1989]. Unfortunately, there is no good supporting data to judge the validity of any of these estimates.

One may have noticed that, in the two examples above, a single encroachment angle is used to estimate the expected size of the hazard envelope with Eq. (7), instead of using the entire distribution of the encroachment angle. This has been practiced by many studies, e.g., SR214 [TRB, 1987] and Daily et al. [1997]. This poses an important question as to what a good choice of f value would be if one is to choose one value to estimate the average or expected size of H_q using Eq. (7). One observation made from the simulations above was that, when $\ell_{obj,q}$ is short, plugging-in the average encroachment angle in Eq. (7) is not a good estimate of the average size of envelope. For example, in the guardrail example, if one uses the average angle 8.5° in Eq. (7), the average size of the envelope would be estimated as 1,387 ft (which is about 7 percent lower than the actual average envelope (1,493 ft) estimated from the simulation. However, in the utility pole example, the estimate would be 66 ft, which is about 60 percent lower than the actual average envelope of 168 ft. The reason for the underestimation is that the distribution of f is skewed to the right (with a positive coefficient of skewness) and the size of the envelope is a nonlinear function of f . If the average encroachment angle is not a good choice, what f value should be used to estimate the expected size of H_q using Eq. (7)? This particular question did not seem to be addressed by earlier studies when estimating the size of the envelope for point objects, such as sign posts and utility poles [TRB, 1987; Daily et al., 1997]. The validity of these practices is, therefore, questionable.

Note that the expected size of H_q , which is represented analytically as

$\int_{f_{\min}}^{f_{\max}(v)} \int_{v_{\min}}^{v_{\max}} [\ell_{obj,q} + W_{obj,q} \cot(f) + W_{veh} \csc(f)] f(v, f) dv df$, does not exist if $f_{\min}=0$. This is the reason $f_{\min}=0.25^\circ$ was used instead of 0° in previous simulations. The choice of $f_{\min}=0.25^\circ$ is arbitrary; it is simply chosen to represent a very small encroachment angle.

Process 3

Process 3 determines $P(C_q | In H_q, v, f, X^{(3)})$, the probability that if the vehicle encroaches and is in H_q , the vehicle will collide with the object. As indicated in Figure 1, many factors are involved in this process, including roadside, vehicle, and driver conditions. The main roadside conditions that have been considered in the encroachment-based studies are lateral offset of the object, D_{obj} , and surface type, slope, and wetness. These determinants are also recognized as the key roadside variables by the accident-based studies [Zegeer et al., 1987; Zegeer et al., 1990; Miaou, 1996]. It is obvious that D_{obj} can vary from object to object, which will therefore be denoted by $D_{obj,q}$. The main vehicle conditions identified by the encroachment-based studies include vehicle braking system and tire condition, while the main driver variables identified include the driver's response delay (to the occurrence of roadside encroachment) and the driver's braking and steering behavior after the vehicle encroaches. As mentioned earlier, this is the process where research results in vehicle dynamics and driver behavior (including maneuvering characteristics and in-vehicle habits) can potentially be incorporated. For example, the Highway Vehicle Object Simulation Model is a sophisticated vehicle-handling simulation model that has been used in some encroachment-based studies [Mak and Sicking, 1992; Mak and Bligh, 1996]. Note that, depending on the focus of the study, the choice of the level of analytical complexity for modeling this process is oftentimes at the discretion of the analysts.

To illustrate the concept, simple kinematic equations will be presented here. These equations have been used to estimate time to collision and impact speed for a given encroachment speed and angle with the assumptions that encroachment trajectory is a straight line and deceleration rate is a constant [Mak and Sicking, 1992]. Table 1 shows these equations under different encroachment conditions. In these equations, the lateral offset, D_{obj} , is the key roadside variable that is explicitly modeled, while surface type, slope, and wetness are implicitly modeled through the choice of vehicle deceleration rate (D). Vehicle braking system and tire condition are also implicitly represented via the choice of D . Driver response delay, t_r , is explicitly considered, while braking behavior is remotely implied in the choice of D . Steering behavior, on the other hand, is ignored completely. Despite their simplicity, these equations do capture a simple crash-avoidance maneuver very well at the conceptual level and can serve as a basis for considering more complicated maneuvers.

In theory, one can choose t_r from a distribution function that represents the probability of a driver's response delay in typical roadside encroachment circumstances due to the driver's temporary inattentiveness, as well as in extreme cases where a driver falls asleep completely. The data to calibrate this distribution function are, however, not available and have not been considered in the data collection plans mentioned earlier.

It is worth pointing out that ignoring a driver's ability to make steering correction is a critical limitation, since most of the encroachments are expected to have small encroachment angles and, under such encroachments, the alerted driver can usually apply a combination of braking and steering operations to swerve the vehicle back into the travel lane before hitting any object.

Clearly, the effects of many factors are being lumped together and implied in a simple variable, D . Without additional modeling effort, it will be difficult, and possibly meaningless, to suggest a probability distribution function for D . Intuitively, D is highly dependent on the roadside surface condition, especially sideslope ratio, which is of great interest to this study. By limiting the choice of D to a constant, one can at best assume some sort of ideal braking and roadside surface conditions.

Since a straight-line trajectory is assumed above, the impact angle is the same as the encroachment angle. More complicated trajectories and vehicle yaw rates can, of course, be considered in the process so that a collision is characterized not only by its impact speed, but also by its angle and position of impact. Again, the data to support these more complicated scenarios are either extremely limited or not available.

Given that an encroached vehicle is in the envelope of an object, additional simulations were conducted to illustrate the conditional probability using the kinematic equations in Table 1. In these simulations, new parameters were set: $t_r=1$ sec and $D=0.5 g=16.1 \text{ ft/sec}^2$. These parameters represent an alerted driver and a car encroaching on a relatively flat surface with a good tire-surface friction coefficient. Lateral offsets, D_{obj} , are set for 0, 5, 10, 15, 20, ..., 50 ft at different simulation runs. Given v, f , constants t_r and D , and the encroachment location within H_q , the impact speed associated with the q th object, $V_{c,q}$, can be computed deterministically using the equations in Table 1. Figure 4 shows the distribution of impact speeds as a result of

different encroaching speeds, angles, and locations within H_q . Analytically, Figure 4 shows the collision probability $P(C_q | In H_q, X^{(3)}) = \int_{\mathbf{f}} \int_{\mathbf{v}} P(C_q | In H_q, \mathbf{v}, \mathbf{f}, X^{(3)}) f(\mathbf{v}, \mathbf{f}) d\mathbf{v} d\mathbf{f}$.

Figure 4(a) shows that the percentage of vehicles that hit the object decreases as the lateral offset of the object increases. For those that impact the object, Figure 4(b) further shows the distributions of their impact speed for different lateral offsets of the object. It was noted that the rate of decrease in collision probability in Figure 4(a) is almost a constant, but it is not as pronounced as those used in the current *Roadside Design Guide* and that estimated in Miaou [AASHTO, 1989; Miaou, 1996; Miaou, forthcoming]. Note that Miaou assumed an exponential rate of decrease for a roadside surface that is relatively flat and showed that the results are quite consistent with those used in the *Roadside Design Guide* [AASHTO, 1989; Miaou, 1996]. Of course, there are many possible explanations for their discrepancies, such as the simplification of behavior models in the simple kinematic equations.

Combining Processes 2 and 3

Both Processes 2 and 3 are conditional on \mathbf{v} and \mathbf{f} . To understand the analytical property of these two processes jointly, Monte-Carlo simulations were conducted for different sizes of point objects and for various lengths of continuous objects. Mathematically, the simulation seeks to understand the following process:

$$\begin{aligned} P(C_q | \mathbf{x}, X^{(2)}, X^{(3)}) &= \int_{\mathbf{f}} \int_{\mathbf{v}} P(C_q | \mathbf{x}, \mathbf{v}, \mathbf{f}, X^{(2)}, X^{(3)}) f(\mathbf{v}, \mathbf{f}) d\mathbf{v} d\mathbf{f} \\ &= \int_{\mathbf{f}} \int_{\mathbf{v}} P(In H_q | \mathbf{x}, \mathbf{f}, X^{(2)}) P(C_q | In H_q, \mathbf{v}, \mathbf{f}, X^{(3)}) f(\mathbf{v}, \mathbf{f}) d\mathbf{v} d\mathbf{f} \end{aligned} \tag{9}$$

Eq. (8) and the simple kinematic equations in Table 1 are used in the simulation. Again, the simulations were conducted for different lateral offsets of the object. The length of the road section is fixed and set to $L = 1$ mi (5,280 ft).

For the simulations of point objects, two round-shaped objects of the same lateral offset, one on each side of the road, are considered. The simulations were conducted for various sizes of the object, ranging from 4 inches to 12 inches in diameter. Figure 5 shows the collision probabilities by lateral offsets and by size of the object. Figure 5(a) shows that the probability decreases

monotonously as the lateral offset increases. Additional computations revealed that the percentage decrease in collision probability is not a constant; it decreases drastically initially and becomes a constant as the lateral offset increases. This suggests that, for a particular type of point object considered (of the same size), an exponential function of the lateral offset is a good candidate function to represent the collision probability. However, within the exponential function, the coefficient associated with the lateral offset may have to change as the lateral offset increases. Thus, within the exponential function, either a second or higher order polynomial function or a step function of the lateral offset (which will be described in the next section) may have to be considered. Figure 5(b) indicates that, for a fixed lateral offset, the probability of a collision increases in a linear fashion as the size of the object increases. More specifically, the probability of a collision increases in a linear fashion as the average size of the hazard envelope increases (not shown in the figure).

For the simulations of continuous objects, two objects of the same lateral offset, one on each side of the road, are again considered. The widths of the objects are set to a constant ($W_{obj,q}=1$ ft) and length $\ell_{obj,q}$ varies from 100 ft to 2,500 ft. Figure 6 shows the same probabilities as those presented for the point objects. Figure 6(a) shows that the probability of a collision decreases as the lateral offset increases. As in the point object simulations, an exponential function of the lateral offset is a good candidate function to represent the collision probability. An interesting observation is that, for $\ell_{obj,q} \geq 750$ ft, the rate of decrease in collision probability appears to be fairly constant as the lateral offset increases. This suggests that, within the exponential function, a simple linear function of the lateral offset with one coefficient will suffice for representing the collision probability when $\ell_{obj,q} \geq 750$ ft. As the length of the object becomes shorter (relative to 750 ft), the percentage decrease in collision probability deviates further from a constant. And, as the length becomes very small, the percentage decrease in collision probability decreases drastically initially and becomes a constant as the lateral offset increases. As in the point object, to model the collision probability for short continuous objects, a second or higher order polynomial function or a step function of the lateral offset becomes necessary within the exponential function. Also, Figure 6(b) indicates that, for a fixed lateral offset, the probability of a collision increases in a linear fashion as the size of the object (or, more precisely, the size of hazard envelope) increases.

Output of Process 3

One of the key outputs from Process 3 is an impact speed. If the impact speed is greater than zero (i.e., an object is hit), then it serves as input to Process 4.

Process 4

Process 4 determines $P(A_q | C_q, f, v, X^{(4)})$. As mentioned earlier, in a more sophisticated vehicle trajectory model, the collision is characterized by impact speed, impact angle, and the position of impact. However, in previous studies, very simple conditional probabilities have been assumed based on limited data and some engineering judgment. For example, a constant probability of 0.9 was used for hitting utility poles in SR214. A more sensible way would be to determine the probability based on the impact speed (or the lateral offsets of objects since the impact speed is a function of lateral offsets). For simplicity, the impact speed is the only collision characteristics considered in this study. To make the impact speed explicit in the conditional probability, we can write $P(A_q | C_q, V_{c,q}, X^{(4)})$, instead of $P(A_q | C_q, f, v, X^{(4)})$. This probability has to be determined for each type of object. For example, it may be decided that if the impact speed with a utility pole is greater than 5 mph, then it will result in a reportable accident. That is,

$$\begin{aligned} P(A_q | C_q, V_{c,q}, X^{(4)}) &= 1 && \text{if } V_{c,q} > 5 \text{ mi / hr} \\ &= 0 && \text{otherwise} \end{aligned} \tag{10}$$

The choice of the threshold impact speed is, of course, dependent on the nature of the object considered (e.g., the material of which the object is made).

Similar to the setup of the last simulations, a simulation was conducted to gain some understanding of the probability when different thresholds of $V_{c,q}$ are chosen. Figure 7 shows the probabilities for an 8-inch diameter point object and a 0.25-mile continuous object. Naturally, the probability decreases as a higher threshold value of $V_{c,q}$ is chosen. However, the simulation results suggest that the decrease in probability is very small when $V_{c,q}$ increases from 0 to 10 mi/hr. Another interesting observation is that, for a given threshold value of $V_{c,q}$, the decrease in collision probability remains very much the same as the lateral offset increases.

The severity of accidents is expected to be some function of impact speed. Therefore, this is the process where the conditional probability of various accident severity levels could potentially be considered. Conceivably, crash test results, which can be computer simulated, can potentially be used to determine the relationship between severity and impact speed. Also, this is the process where the changes of safety features in vehicle population can be reflected, such as the percentages of vehicles equipped with airbags and dynamic side-impact protection and the rate of seat-belt use.

Overall Probability and Expected Number of Accidents

Provided that the overlapping of H_q can be properly accounted for (or avoided), the probability of an encroached vehicle to be involved in an accident with one of the objects on the road, symbolized by A , is the sum of the probability over all objects:

$$\begin{aligned}
 & P(A|\mathbf{x}, X^{(2)}, X^{(3)}, X^{(4)}) \\
 &= \sum_{q=1}^Q \left[\int_{\mathbf{f}} \int_{\nu} P(A_q | \mathbf{x}, \nu, \mathbf{f}, X^{(2)}, X^{(3)}, X^{(4)}) f(\nu, \mathbf{f}) d\nu d\mathbf{f} \right] \\
 &= \sum_{q=1}^Q \left[\int_{\mathbf{f}} \int_{\nu} P(InH_q | \mathbf{x}, \nu, \mathbf{f}, X^{(2)}) P(C_q | InH_q, \nu, \mathbf{f}, X^{(3)}) P(A_q | C_q, \nu, \mathbf{f}, X^{(4)}) f(\nu, \mathbf{f}) d\nu d\mathbf{f} \right]
 \end{aligned} \tag{11}$$

As stated earlier, in the encroachment-based studies, it is expected that the (expected) encroachment rate can be pre-determined based on mainline conditions. The encroachment rate, denoted by R_x , is typically given as the number of encroachments per million vehicle-miles traveled. Given R_x and all determinants, the expected number of accidents on the road section in N years is calculated as

$$\begin{aligned}
 & E[Y | X^{(1)}, Z^{(1)}, X^{(2)}, X^{(3)}, X^{(4)}] = \\
 & \quad (365 \times N \times AADT \times L / 10^6) \times R_x \times P(A|\mathbf{x}, X^{(2)}, X^{(3)}, X^{(4)})
 \end{aligned} \tag{12}$$

where Y is the number of reportable accidents involving the type of objects, L is in miles, $AADT$ is in number of vehicles, and $(365 \times N \times AADT \times L / 10^6) \times R_x$ is the expected total number of encroachments during the period. One of the basic encroachment parameters of interest is the

expected encroachment frequency per mile per year. If R_x is estimated and symbolized as \hat{R}_x , then the encroachment frequency can be obtained as $(365 \cdot AADT / 10^6) \cdot \hat{R}_x$. An implicit assumption used here is that the RORA experiences of individual drivers traveling through the section are independent from one another (which is a reasonable one).

FORM OF MEAN FUNCTIONS

Unlike the encroachment-based approach, the accident-based approach deals with one conditional probability only: the probability of having y accidents, given the available determinants, or mathematically, $P(Y = y | X^{(1)}, Z^{(1)}, X^{(2)}, X^{(3)}, X^{(4)})$, where $y = 1, 2, 3, \dots, \infty$.

There are basically five major tasks in developing accident-based models: (1) find a good probability (mass) function to describe the random variation of accident frequency; (2) determine an appropriate functional form and parameterization for the mean function which describes the effect of key variables on accident frequency; (3) select the variables that have statistically significant effects on accident frequency for inclusion in the mean function; (4) estimate the regression parameters in the mean function and obtain good statistical inferences for the estimated parameters based on available data; and (5) assess the quality of the model; judge whether the developed model makes good engineering sense; decide whether the developed model meets the planning and design requirements; and identify cost-effective ways to improve the model. The work involved in each of these tasks has been described in Miaou [1996]. Since the theory behind the Poisson and NB regression accident-based models have been discussed quite extensively in many recent publications [Maycock and Hall, 1984; Miaou et al., 1993; Miaou and Lum, 1993; Miaou, 1994; Maher and Summersgill, 1996; Miaou, 1996], the readers are referred to these publications for a review of these models.

As seen in the last section, the focus of the encroachment-based model has been on the second task, determining the appropriate functional form and parameterization for the mean function and on identifying key determinants. In this section, several mean functions will be formulated for use in the accident-based models, following the encroachment-based thinking described in the last section. Specifically, the objective is to determine mean functions based on Eqs. (11) and (12) and simulation experience gained in the last section.

As stated earlier, the encroachment-based thinking described above does not provide any engineering insights on what the plausible functional forms of $P(x|X^{(1)}, Z^{(1)})$ might be. Thus, it does not provide any clue as to the functional form of R_x in relation to $X^{(1)}$ and $Z^{(1)}$. It has been argued in the accident-based literature that a plausible functional form should be multiplicative in nature and represent the interactive effects of various mainline design and traffic variables on accident frequency. The exponential form has been suggested to be a good candidate because it is simple and it ensures that the expected value will always be non-negative [Miaou, 1996]. By applying the same argument to the encroachment frequency, we can express the encroachment rate as

$$R_x = \exp(b_1^* + \sum_{j=2} b_j x_{ij} + \sum_k g_k z_{ik}) \quad (13)$$

where, for clarity, the subscript i introduced to represent the road section being considered is the i th section in the sample road sections; x_{ij} is the value of the available mainline design and traffic variables for the i th road section; z_{ik} is the value of the unobservable variables for the section; and b_1^* , b 's, and g 's are unknown model parameters. Note that, when appropriate, higher order and interactive terms of the covariates can be easily included in Eq. (13).

The encroachment-based thinking described in the last section does provide some good ideas on the choice of the functional form in Eq. (11). One such choice, which is consistent with the simulation results shown in Figures 5-7, would be

$$P(A|\ell_{obj}, W_{obj}, D_{obj}) = \prod_{q=1}^Q \frac{\hat{e}^{\ell_{obj,q} + d_q}}{2L} \left[\exp(a_1 D_{obj,q} + a_2 D_{obj,q}^{(1)} + a_3 D_{obj,q}^{(2)} + \dots) \right] h_v \quad (14)$$

where d_q is the part of the hazard envelope associated with vehicle swath width, object width, and adjustments for the overlapping of envelopes; a polynomial or a step function of $D_{obj,q}$ is used within the exponential function to model collision probabilities (as suggested from the previous simulations); a 's are unknown parameters associated with the polynomial function; and h_v is associated with the threshold impact speed discussed earlier and is a constant between

0 and 1. When $h_v=1$, it indicates that any impact speed greater than 0 will result in an accident. According to the simulation results shown in Figure 7, h_v should be fairly close to 1 if the threshold impact speed is less than 10 mi/hr. Thus, for typical non-breakaway, fixed objects, if we are interested in all reportable accidents (regardless of their severity) a reasonably good estimate of h_v would be close to 1 and can be determined outside of the accident model.

Note that, to use a polynomial function of $D_{obj,q}$ in Eq. (14), $D_{obj,q}^{(1)} = D_{obj,q}^2$, $D_{obj,q}^{(2)} = D_{obj,q}^3$, and $D_{obj,q}^{(3)} = D_{obj,q}^4$, etc., and, for a step function, $D_{obj,q}^{(1)} = D_{obj,q}$, if $D_{obj,q}$ is greater than a predetermined distance, e.g., 5 ft, otherwise a zero is assigned; $D_{obj,q}^{(2)} = D_{obj,q}$, if $D_{obj,q}$ is greater than a larger predetermined distance, e.g., 10 ft, otherwise a zero is assigned; and $D_{obj,q}^{(3)} = D_{obj,q}$, if $D_{obj,q}$ is greater than another larger predetermined distance, e.g., 15 ft, otherwise a zero is assigned, etc. The step function so arranged would allow the rate of decrease in collision probability to change in a step-wise manner as the lateral offset increases. For the example step function here, the percent decrease in collision probability is approximately - $100a_1\%$ per foot increase in $D_{obj,q}$ when $D_{obj,q}$ is between 0 and 5 ft, - $100(a_1 + a_2)\%$ when $D_{obj,q}$ is between 5 and 10 ft, and - $100(a_1 + a_2 + a_3)\%$ when $D_{obj,q}$ is between 10 and 15 ft, etc.

In Eq. (14), $D_{obj,q}$ is the only roadside design variable considered in determining collision probability after roadside encroachments occur. As indicated earlier, sideslope and surface types are two other key variables that were implicitly considered in the simulations presented earlier. Thus, a plausible extension of Eq. (14) is to add sideslope as the second roadside design variable within the exponential function on the right-hand side of Eq. (14). However, a representative sideslope may be difficult to obtain for two reasons: (1) the sideslope can vary significantly within a road section, and (2) for a particular object, the sideslopes of interest are the slopes that are located within the hazard envelope of the object, the location and size of which also need to be estimated. Also, to reflect the difference in the friction coefficient of different surface types, such as paved and unpaved shoulders, in the model, the lateral offset, $D_{obj,q}$, can be provided by surface type and the model parameter associated with the lateral offset can vary from one surface type to another.

Substituting Eqs. (13) and (14) into Eq. (12), we have a general mean function for the accident-based models for both point and continuous objects.

$$E[Y | X^{(1)}, X^{(2)}, X^{(3)}, X^{(4)}] = \left(365 \times N \times AADT \times L / 10^6 \right) \times \exp(\mathbf{b}_1 + \sum_{j=2} \mathbf{b}_j x_{ij}) \times \left\{ \sum_{q=1}^Q \left[\frac{\ell_{obj,q} + \mathbf{d}_q}{2L} \right] \left[\exp(\mathbf{a}_1 D_{obj,q} + \mathbf{a}_2 D_{obj,q}^{(1)} + \mathbf{a}_3 D_{obj,q}^{(2)} + \dots) \right] \mathbf{h}_v \right\} \quad (16)$$

where \mathbf{a} 's, \mathbf{b} 's and \mathbf{g} 's are unknown model parameters to be estimated from the data. It should be noted that the term $\exp(\hat{\mathbf{a}}_k \mathbf{g}_k \mathbf{z}_{ik})$ has been taken out of the expectation since the variable $\mathbf{Z}^{(1)}$ is not available in practice. Using the Poisson assumption for the randomness of accident frequency, together with the assumption that the exponential function of the unobservable variables (i.e., $\exp(\hat{\mathbf{a}}_k \mathbf{g}_k \mathbf{Z}_{ik})$) is gamma distributed with an expected value of one, a negative binomial regression model can be derived with Eq. (16) as its mean function [Miaou, 1996]. These two assumptions are quite plausible and flexible for count data analysis. They have been used in accident-based models and widely accepted in other fields such as biostatistics and econometrics.

In Eq. (16), \mathbf{d}_q is a variable that varies over individual object. If overlapping of hazard envelopes, i.e., the size of $OL_q(f)$, is judged to be small, then \mathbf{d}_q can be treated as a constant, say \mathbf{d} . More discussion on the estimation of \mathbf{d}_q will be provided in the following paragraphs. Also, as indicated earlier, the simulation results presented in Figure 7 suggested that, when non-breakaway, fixed objects are considered, $\mathbf{h}_v = 1$ is a good estimate and can be determined outside of the accident-based model if all reportable accidents are of interest. Note that, after the model parameters in Eq. (16) are estimated, the expected encroachment frequency per mile per year can be obtained for a given set of covariate values, \mathbf{x}_{ij} , as:

$$\left(365 \times AADT / 10^6 \right) \exp(\hat{\mathbf{b}}_1 + \sum_{j=2} \hat{\mathbf{a}}_j \hat{\mathbf{b}}_j x_{ij}), \text{ where } \hat{\mathbf{b}} \text{'s are estimated parameters.}$$

For point objects where the overlapping of hazard envelopes is small, d_q is approximately a constant, represented by d . Also, $\ell_{obj,q}$ is considerably smaller than d and can be ignored. Under these conditions, Eq. (16) becomes

$$\begin{aligned}
 E[Y | X^{(1)}, X^{(2)}, X^{(3)}, X^{(4)}] \approx & \\
 & (365 \times N \times AADT \times L / 10^6) \times \exp(\mathbf{b}_1 + \sum_{j=2} \mathbf{b}_j x_{ij}) \\
 & \times \left\{ \frac{Qd}{2L} \sum_{q=1}^Q w_q \left[\exp(\mathbf{a}_1 D_{obj,q} + \mathbf{a}_2 D_{obj,q}^{(1)} + \mathbf{a}_3 D_{obj,q}^{(2)} + \dots) \right] \mathbf{h}_v \right\}
 \end{aligned} \tag{17}$$

where Qd is the total length of the hazard envelopes associated with the Q objects along the road section, $w_q = 1/Q$ represents the fraction of the total hazard envelopes that is associated with the q th object and $\sum_{q=1}^Q w_q = 1$. The two parameters d and b_1 in the equation cannot be uniquely determined from the estimation procedure of the accident-based model. In order to estimate b_1 , which is required if the encroachment rate is to be estimated from the model, d has to be determined outside of the accident-based model. However, recall that, even if the vehicle swath width is set to be a constant of 9 ft, d can still vary significantly over different choices of f – 168 ft according to the previous utility pole simulation, about 69.4 ft when using Hutchinson and Kennedy’s [1966] encroachment angle, and about 36.8 ft when using the encroachment angle recommended by *Roadside Design Guide* [1989]. (Note that h_v is again assumed to be determined outside of the accident-based model.) One important observation to be made from Eq. (17) is that a good estimate of b_1 not only requires a good estimate of d , but also requires the functional form of the effect of $D_{obj,q}$ on collision probability be appropriately specified from the data, especially for the range where $D_{obj,q}$ is close to zero.

For relatively long continuous objects, $\ell_{obj,q}$ (say, greater than 750 ft) will be considerably larger than d_q . Thus, Eq. (16) can be approximated by

$$\begin{aligned}
E[Y | X^{(1)}, X^{(2)}, X^{(3)}, X^{(4)}] \approx & \\
& (365 \times N \times AADT \times L / 10^6) \times \exp(\mathbf{b}_1 + \sum_{j=2} \mathbf{b}_j x_{ij}) \\
& \times \left\{ \frac{L_{obj}}{2L} \sum_{q=1}^Q w_q [\exp(\mathbf{a}_1 D_{obj,q})] \mathbf{h}_v \right\}
\end{aligned} \tag{18}$$

where $L_{obj} = \dot{\mathbf{a}}_{q=1}^Q \ell_{obj,q}$ is the total length of the object on both sides of the road section and $w_q = \ell_{obj,q} / L_{obj}$ represents the fraction of the total hazard envelopes that is associated with the q th object and $\dot{\mathbf{a}}_{q=1}^Q w_q = 1$. Note that in Eq. (18), based on the simulation results presented earlier, a constant rate of decrease for the collision probability as $D_{obj,q}$ increases is adopted and the parameter $\mathbf{a}_1 < 0$. Unlike the point object, \mathbf{b}_1 can be determined with good accuracy without requiring a good estimation of d to be obtained (if \mathbf{h}_v is determined externally as stated earlier).

The discussion above suggested that there are several advantages of using long continuous objects to develop accident-based models for estimating encroachment rates over the use of point or short continuous objects:

- (1) For long continuous objects, good estimates of encroachment rates do not require good estimation of d . For short continuous and point objects, the accuracy of the estimation of encroachment rates is directly dependent on the estimation of d , which could be off by a factor of 4.5, depending on which encroachment angle is assumed. Also, a good estimate of the encroachment rate will require the functional form of the effect of $D_{obj,q}$ on collision probability be appropriately specified from the data, especially for the range where $D_{obj,q}$ is close to zero.
- (2) For the same reason stated above, the overlapping of hazard envelopes is less of a problem in estimating model parameters when long continuous objects is considered (when compared to short continuous and point objects).
- (3) The simulation in this study suggested that, for long continuous objects (e.g., ≥ 750 ft [229 m]), a simple exponential function of the lateral offset is sufficient to represent the collision

probability, and more complicated functions of the lateral offset will be required if short continuous or point objects are considered.

- (4) If the sideslope is to be considered as a determinant of the collision probability, given an encroachment, it will be a lot more difficult to obtain a representative sideslope for point and short continuous objects than for long continuous objects. This is because the sideslopes of interest are the slopes that are located within the hazard envelope of the object, the location and size of which need to be estimated. And, as indicated earlier, better estimates of the size of hazard envelopes can be obtained for long continuous objects than for short continuous or point objects.

ESTIMATING ENCROACHMENT RATES

This section is intended to show how accident-based models can be useful to the encroachment-based models. Specifically, roadside encroachment rates for rural, two-lane, undivided roads will be estimated using the accident-based model. The candidate mean functions suggested in the last section will be employed in developing the accident-based models for accidents involving guardrails and utility poles.

Accidents and roadway data for rural, two-lane, undivided roads from a roadway cross-section design data base [Rodgman et al., 1989] administered by FHWA were used to develop accident-based models. This data base contains 1,944 road sections, most of which are located in rural areas. Specifically, out of the 1,944 sections, about three-quarters of them can be considered to be truly rural, undivided roads. One of the important features of this particular data base is that it contains a rather detailed description of key design elements of various roadside obstacles. This data base has been used in previous studies to develop accident-based models for rural, two-lane, undivided roads, such as Zegeer et al. [1987], Zegeer et al. [1990], and Miaou [1996]. A good description of the data collection process and general statistics of the road sections included in this data base can be found in Rodgman et al. [1989] and Zegeer et al. [1990]. The road sections contained in the data base represent a stratified random sample from seven States: Alabama, Michigan, Montana, North Carolina, Utah, Washington, and West Virginia. Except for Alabama, which has about 2.5 years worth of data, five years of accident data from 1980 to 1984 were available for analysis. Note, however, that accident data were not broken down by year.

For each road section, the data base has the inventory of roadside objects within 30 ft of the edge line of travel lanes.

Guardrail Accidents

Only those road sections with guardrails in the data base are of interest. For each road section in the data base, the total number of miles of guardrails (or guardrail-miles) is recorded according to the clear zone width (or lateral offsets). However, in the data base, clear zone widths are grouped into eight categories: < 1.5 ft, 1.5 to 3.5 ft, 3.5 to 6.5 ft, 6.5 to 10.5 ft, 10.5 to 15.5 ft, 15.5 to 20.5 ft, 20.5 to 25.5 ft, and 25.5 to 30 ft. That is, for each clear zone width category within each road section, we have the total guardrail-miles, but we don't know how many disjointed guardrails have been included. We also do not know their relative positions within the road section and how many are on the left and right sides of the road. Note that, for those guardrails that fall into different clear zone width categories, we do know for sure that they are disjointed. Also, for the modeling purpose, the mid-point of each clear zone width category is used to represent the clear zone width for all guardrails located in this category.

Recall that in order to use Eq. (18) as the mean function, we need to be able to select road sections with relatively long guardrails. Specifically, we need $\ell_{obj,q}$ to be considerably larger than d_q . Also, recall that d_q is about 173 ft (if hazard envelopes are not overlapped), according to the simulation presented earlier, and is much smaller if the encroachment angle from *Roadside Design Guide* [AASHTO, 1989] or Hutchinson and Kennedy [1966] are used. For the reasons stated in the last paragraph, in this data base, we will never be certain that we have included only road sections with long guardrails. However, the probability that most of the road sections that are included have long guardrails should increase if we choose to remove more road sections with short guardrail-miles. On the other hand, we clearly need to have a reasonably large sample size to develop meaningful statistical models.

To compromise, road sections with guardrail miles less than 0.1 mi (or about 0.16 k) per side of road were first removed, leaving 272 road sections for analysis. The length of these sections ranges from 1 to 9.37 mi, with an average length of about 3 miles (4.8 k). The total length of these road sections is 841 mi, while the total guardrail-miles is about 109 mi per side of road. During the period considered, there were 450 recorded guardrail accidents on these road

sections, regardless of vehicle and accident severity type. With the total vehicle-miles estimated to be 3,486 million and vehicle guardrail-miles traveled estimated to be 471 million, the overall guardrail accident rate was 0.12 accidents per million vehicle-miles traveled and 0.96 accidents per million guardrail-miles traveled. Note that the rate is calculated assuming that guardrail-miles are equally distributed on both sides of the road. Of the 272 road sections, about 43% of them (118 sections) had no recorded guardrail accident. The maximum number of guardrail accidents recorded for an individual road section was 19 during the 5-year period.

Of the 109 guardrail-miles per side of the road, their distribution across the eight clear zone width categories were: 1.37%, 14.31%, 36.88%, 34.74%, 11.96%, 0.60%, 0.06%, and 0.08%, respectively. That is, the majority of the guardrail-miles are located in categories 2 to 5 or between 1.5 to 15.5 ft. For these 272 road sections, in addition to vehicle-miles traveled (in millions), other covariates considered and their associated ranges are as follows:

- AADT per lane, used as a surrogate measure for traffic density; AADT is between 160 and 10,000 vehicles per day.
- Lane width: Between 9 and 13 ft.
- Horizontal curvature: Non-homogeneous within a section, i.e., each section may contain multiple curves; length-weighted horizontal curvature is between 0 and 21 degrees/100 ft arc.
- Vertical grade: Non-homogeneous within a section, i.e., each section may contain multiple grades; length-weighted vertical grade is between 0 and 8 percent.
- Clear zone width (or lateral offset), measured from the outside edges of travelway to the guardrail, which includes:
 - ◇ paved shoulder width, Between 0 and 12 ft,
 - ◇ unpaved shoulder width (i.e., earth, grass, gravel, or other stabilized shoulder width), Between 0 and 10 ft,
 - ◇ additional clear zone width beyond shoulders, Between 0 and 6.2 ft.

About 90% of the road sections have shoulders that are either paved or unpaved, i.e., only about 10% of the road sections have a mixed shoulder type. Also, about 90% of them have a posted speed limit of 55 mi/hr. In addition, about 12% of the sample road sections do not have

horizontal curvature data, and about 21% do not have vertical grade data. Furthermore, most of the road sections have 11 ft as the lane width.

Guardrail accident models were developed using these 272 road sections, as well as two subsets of these sections, in which road sections with longer guardrail-miles (> 0.15 mi or 792 ft and > 0.2 mi or 1,056 ft per side of road) were selected. The total numbers of road sections available for developing models for the two subsets were 217 and 188 sections, respectively.

An extended NB regression model, as described in Miaou [1997], was employed in this study. The model is a general-purpose model which allows mean functions to have the form as shown in Eqs. (17) and (18). To be more specific, for each road section i , the conventional NB regression has a multiplicative mean function of the following form:

$$\begin{aligned}
 E[Y_i | v_i, x_{ij}, j = 1, 2, \dots, J] &= v_i \exp\left(\sum_{j=1}^J \mathbf{b}_j x_{ij}\right) \\
 &= v_i \exp(\mathbf{b}_1 x_{i1}) \exp(\mathbf{b}_2 x_{i2}) \cdots \exp(\mathbf{b}_J x_{iJ}) \\
 &= v_i \left[\prod_{j=1}^J \exp(\mathbf{b}_j x_{ij}) \right]
 \end{aligned} \tag{19}$$

where v_i is typically called an offset of the model (which usually represents an exposure measure in the accident-based model), x_{ij} is the value associated with the j th covariate of the road section i , and \mathbf{b}_j is a regression parameter associated with the j th covariate. That is, in the conventional NB regression model, the effect of covariate j on the expected number of accidents is modeled as a simple exponential function of the form: $\exp(\mathbf{b}_j x_{ij})$.

In the extended NB model, the effect of the j th covariate on the mean function is allowed to have the following form:

$$\prod_{s=1}^{S_{ij}} w_{ijs} \exp\left(\prod_{k=1}^{K_j} \mathbf{b}_{kj} x_{ijsk}\right) \tag{20}$$

where w_{ijs} represents a predetermined weight associated with a subsection s ($=1, 2, \dots, S_{ij}$) of road section i , x_{ijsk} , $k=1, 2, \dots, K_j$, are the covariate values that characterize the subsection s , and b_{jk} are unknown model parameters that need to be estimated from the data. Typically, for each road section, we have $\sum_{s=1}^{S_{ij}} w_{ijs} = 1$, i.e., the sum of the predetermined weight over all subsections is equal to 1. The maximum likelihood method is used to estimate unknown model parameters, and the observed Fisher Information Matrix is used to obtain statistical inferences for the estimated parameters.

The mean function in Eq. (20) was formulated specifically to deal with road sections (or sites) that have non-homogeneous attributes along the road section (or within the site). For example, in this study, each road section may have multiple horizontal curvatures and vertical grades, and roadside objects within each road section may have different lateral offsets. To illustrate, here we use the lateral offset of roadside objects in Eq. (17) as an example. That is, the j th covariate is now the lateral offset. Let's say that road section i has S_{ij} roadside objects of interest and their lateral offsets are denoted by $D_{obj,s}$, where $s=1, 2, \dots, S_{ij}$. In this example, w_{ijs} is the fraction of the total hazard envelope that is associated with the s th object. Also, if we use the step function described under Eq. (14) to model the effect of lateral offsets, then $x_{ijs1} = D_{obj,s}$, $x_{ijs2} = D_{obj,s}^{(1)}$, $x_{ijs3} = D_{obj,s}^{(2)}$, etc. Furthermore, in Eq. (17), $v_i = (365 \cdot N \cdot AADT \cdot L / 10^6) \cdot (Qd/2L)$. Note that here, without confusion, the subscript i has been omitted from N , $AADT$, L , Q , and the lateral offset.

The following variable selection procedure was adopted in selecting the final model: Initially, all covariates listed earlier were included in the extended NB regression model and their parameters estimated. Then, the variable that had the least absolute t-statistic value which is less than 1.9 (i.e., not significant at about a 5% significance level) was removed from the model. The parameters of the smaller model were reestimated and their t-statistics reassessed. The procedure continued until the t-statistics of all parameters in the model are greater than about 1.9. Lane width, horizontal curvature, and vertical grade were removed from the model at different stages of the variable selection process. The estimated parameters, as well as their associated standard deviations and t-statistics, of the final selected models are presented in Table 1. Note that AADT

per lane is not statistically significant in the last model presented in the table (for sections with guardrail-miles > 0.2 mi per side of road). This model is presented for comparison purpose only. Also, even though the second and higher order terms (or the step function) of the lateral offset, $D_{obj,q}$, were not required in Eq. (18), as suggested by the simulation, they were still tested in the variable selection procedure and were indeed not found to be statistically significant.

From the three models presented in columns 2-4, it is clear that clear zones have very significant effects on guardrail accident rates. The second and third models (for road sections with guardrail-miles > 0.15 mi per side of road) are preferred because they have a higher probability of excluding road sections with short guardrails. The second model (in column 3) does indicate that different roadside surface types may have different effects on the collision probability. For this particular data set, the difference in their effects is, however, not statistically different. All three models give similar encroachment rates (assuming $h_v=1$ in all three models). Assuming $h_v=1$, the expected numbers of encroachments per mile per year are estimated by AADT using the third model and are shown in Figure 8. The estimates can be seen to be slightly higher than those presented by Miaou [1996], which are also accident-based estimates. The estimates can also be seen to be compatible with those obtained by Hutchinson and Kennedy [1966] and Cooper [1980] which were estimated from field-collected data.

The consistency of these estimates is an indication that estimating basic encroachment parameters using accident-based models, as proposed by Miaou [1996], can be a viable approach to reducing encroachment data collection cost. Most importantly, it is straightforward to use such an approach to estimating basic encroachment parameters for various mainline traffic and design conditions, such as AADT, lane width, horizontal curvature, and vertical grade, when data are available. The only premise is that a sound accident-based model be developed. Another strength of using accident-based models to estimate basic encroachment parameters is that there is no need to develop procedures to distinguish between controlled and uncontrolled encroachments, which, as indicated earlier, can be subjective and technically difficult.

Utility Pole Accidents

This subsection presents the use of utility pole accidents to develop accident-based models and estimate roadside encroachment rates. The limitations described earlier regarding the use of

point objects to estimate encroachment rates are then illustrated. Note that due to a serious limitation of the utility pole data contained in the data base, which will be described later, the utility pole accident-based models presented in this subsection are not considered to be reliable and are for illustration purpose only.

Only those road sections with utility poles in the data base are of interest. As in the guardrail data, the total number of utility poles is inventoried by eight clear zone width categories. For each clear zone width category within each road section, we have the total number of utility poles. However, we do not know their relative positions within the road section and how many are on the left and right sides of the road.

Recall that, in order to use Eq. (17) as the mean function for modeling point object accidents, the overlapping of hazard envelopes has to be small. To reduce the probability of overlapping in hazard envelopes, only road sections with average pole spacing greater than 0.1 mi (528 ft) were considered. Note that the average pole spacing is calculated as two times the section length divided by the total number of utility poles on both sides of the road. Since we do not know the position of these poles, the choice of 0.1 mi is admittedly arbitrary and is mainly based on the simulation results presented earlier where the size of the hazard envelope associated with a utility pole was estimated to be about 168 ft on average.

There were 855 road sections that met the selection criteria. The length of these sections ranges from 0.92 to 9.37 mi, with an average length of 3.02 mi. The total length of these road sections is 2,586 mi, while the total number of utility poles is 20,424 (or 10,212 per side of road). During the period considered, there were 293 recorded utility pole accidents on these road sections, regardless of vehicle and accident severity type. With the total vehicle-miles estimated to be 9,931 million, the overall utility pole accident rate was about 0.03 accidents per million vehicle-miles traveled. Also, there were about 42,211 million vehicle-poles, which gave 0.69 accidents per 100 million vehicle-poles. Note that here a vehicle-pole is defined as a vehicle passing two poles; one on each side of the road, and the rate is calculated assuming that utility poles are equally distributed on both sides of the road. Of the 855 road sections, about 79% of them (673 sections) had no recorded utility pole accident. The maximum number of utility pole accidents recorded for an individual road section was 12 during the 5-year period.

Of the 20,424 utility poles, their distribution across the eight clear zone width categories were: only nine poles (0.05%) in categories 1 and 2, and 313 (1.53%), 1,574 (7.71%), 3,668 (17.96%), 4,412 (21.60%), 4,044 (19.80%), 6,402 (31.35%), respectively, in categories 3 to 8. Thus, very few utility poles (less than 10% of the total) are located within 10.5 ft of the travel lane, about 40% are between 10.5 and 20.5 ft, and over 51% of the poles are located between 20.5 and 30.5 ft. As indicated earlier, a good estimate of b_1 in Eq. (17) not only requires a good estimate of d , but also requires the functional form of the effect of $D_{obj,q}$ on collision probability be appropriately specified from the data, especially for the range where $D_{obj,q}$ is close to zero. With very few utility poles located within 5 ft (or 10 ft) of the travel lane, the model development process has a low probability of success in identifying the appropriate functional form for $D_{obj,q}$ from the data set which, as stated at the outset, is considered a very serious limitation of this data set.

In addition to vehicle-miles traveled (in millions), the following covariates have been considered for individual road sections:

- AADT per lane, used as a surrogate measure for traffic density: AADT is between 160 and 10,000 vehicles per day.
- Lane width: Between 9 and 13 ft.
- Horizontal curvature: Non-homogeneous within a section, i.e., each section may contain multiple curves; length-weighted horizontal curvature is between 0 and 21 degrees/100 ft arc.
- Vertical grade: Non-homogeneous within a section, i.e., each section may contain multiple grades; length-weighted vertical grade is between 0 and 11 percent.
- Sideslope (e.g., 3:1 and 7:1 slopes are recorded as $1/3=0.33$ & $1/7=0.14$, respectively.): Non-homogeneous within a section; length-weighted sideslope is between 0 and 0.91.
- Clear zone width (or lateral offset), measured from the outside edges of travelway to the guardrail, which includes:
 - ◇ paved shoulder width, Between 0 and 11 ft,
 - ◇ unpaved shoulder width (i.e., earth, grass, gravel, or other stabilized shoulder width), Between 0 and 12 ft,
 - ◇ additional clear zone width beyond shoulders, Between 0 and 28 ft.

About 93% of the road sections have shoulders that are either paved or unpaved, i.e., only about 7% of the road sections have a mixed shoulder type. Also, about 93% of them have a posted speed limit of 55 mi/hr. In addition, about 22% of the sample road sections do not have horizontal curvature data, and about 39% do not have vertical grade data. Furthermore, most of the road sections have 11 ft as the lane width.

Several step functions of the clear zone, as described earlier, were also tested in the variable selection process. Column 1 of Table 3 contains a complete list of the covariates considered. Note that, since the position of the poles is unknown, the sideslope measure considered here is more of a characterization of the roadside slope for the entire road section than that for the hazard envelopes encompassed by utility poles.

Recall that a good estimate of the encroachment rate will require the functional form of the effect of $D_{obj,q}$ on collision probability be appropriately specified, especially for the range where $D_{obj,q}$ is close to zero. To illustrate the difficulty of developing the accident-based model with this data set, Table 3 shows three estimated extended NB regression models (in Columns 2 to 4). The first model (Column 2) uses a simple exponential function to model the effect of the clear zone width on collision probability, with different effects for different surface types; the second model (Column 3) uses a simple exponential function of the clear zone width without considering surface types; and the third model (Column 4) uses the step function described earlier. Note that many other models were evaluated and are not presented here. Our overall experience is that when more detailed step functions or higher order functions of the clear zone width were considered, the estimation results tended to become unstable, even with a slight change in the function form or variable definition.

Comparing the estimated regression parameters associated with the clear zone width among the three models in Table 3 suggests that a simple exponential function of the clear zone width will not suffice to model the collision probability, and a more complicated function form will be required. For example, the first model indicates that the estimated parameters are statistically different for the shoulder (0.150.035 for paved shoulders and 0.180.027 for unpaved shoulders and recalled that shoulders are between 0 and 12 ft) and for additional clear zone width beyond the shoulder (0.050.015) at a 5 percent significance level. Also, the parameters of the step

function used in the third model, though not well determined (as seen by their low t-statistics), indicate that the percentage change in collision probability does decrease as the clear zone width increases.

Figure 8 shows the estimated roadside encroachment rates from the first and third models under three different assumptions of the size of d . A wide variation of the estimates can be observed from the figure (even without considering the sampling variations). Because of the limitation of the data set stated earlier, it would not be worth it to dwell on the implications of these models.

DISCUSSION

The effect of underreported minor injury and property-damage-only accidents on model parameter estimation and, in turn, on encroachment rate estimation has not been discussed in this paper. However, it is generally expected that the underreporting probability increases as the severity of accidents decreases. Because the severity of accidents is highly related to the impact speed and, therefore, to the lateral offset of roadside objects, the underreporting probability of accidents is expected to increase as the impact speed decreases or as the lateral offset of objects increases. Under these notions, the parameter a_1 in Eqs. (17) and (18) reflects not only the collision probability, but also the underreporting probability of accidents, as the lateral offset increases. Thus, a higher underreporting rate in the accident data would result in a higher $|a_1|$ value being estimated.

The effect of underreported accidents on parameter b_1 is, however, expected to be relatively small. The reason is that the impact speed and, thus, severity of accidents is expected to be high when vehicles collide with fixed objects that are fairly close to the travel lane (or, more precisely, that have $D_{obj,q}=0$) and, therefore, very few unreported accidents are expected under such collisions. For example, under the joint encroachment speed and angle probability density function used in the Monte-Carlo simulation of this study, when the lateral offset $D_{obj,q}$ is equal to 0, the probabilities of having an impact speed of less than 5, 10, and 15 mi/hr are 0.7%, 2.5%, and 5.9%, respectively, for those vehicles that collide with the object. The small effect of underreported accidents on b_1 suggests that underreporting of minor accidents should have a small effect on encroachment rate estimation when Eqs. (17) and (18) are used.

The research presented in this paper can potentially be extended in several directions:

- (1) Current encroachment-based studies do not provide any clue on what the plausible functional forms for modeling Process 1 (i.e., encroachment probability) might be. Thus, an interesting extension would be to apply traffic flow, driver behavior, and vehicle dynamics theories to gain some engineering insights on this functional form.
- (2) This study used the same data base as in Miaou [1996]. It would be interesting to see if consistent encroachment rates can be estimated when other independent data sets are used.
- (3) In theory, the proposed method for estimating encroachment rates can be extended to consider road sections of roadway classes other than the rural, two-lane, undivided roads.

REFERENCES

1. American Association of State Highway and Transportation Officials (AASHTO) (1989) *Roadside Design Guide*. Washington, D.C.
2. Cooper, P. (1980) *Analysis of Roadside Encroachments^{3/4}Single Vehicle Run-Off-Road Accident Data Analysis for Five Provinces*. B.C. Research, Vancouver, Canada.
3. Daily, K., Hughes, W., and McGee, H. (1997) *Experimental Plans for Accident Studies of Highway Design Elements: Encroachment Accident Study*. FHWA-RD-96-081. FHWA, U.S. Department of Transportation.
4. Fancher, P., Kostyniuk, L., Massie, D., Ervin, R., Gilbert, K., Reiley, M., Mink, C., Bogard, S., and Zoratti, P. (1994) *Potential Safety Applications of Advanced Technology*. FHWA-RD-93-080. FHWA, U.S. Department of Transportation.
5. Glennon, J.C. (1974) *Roadside Safety Improvement Programs for Freeways^{3/4}A Cost Effectiveness Priority Approach*. National Cooperative Highway Research Program, Report 148, Transportation Research Board. Washington, D.C.
6. Hutchinson, J.W. and Kennedy, T.W. (1966) *Medians of Divided Highways^{3/4}Frequency and Nature of Vehicle Encroachments*. Engineering Experiment Station Bulletin 487, University of Illinois.
7. Maher, M.J., and Summersgill, I. (1996) A Comprehensive Methodology for the Fitting of Predictive Accident Models. *Accident Analysis & Prevention*, 28(3): 281-296.
8. Mak, K.K., and Sickling, D.L. (1992) *Development of Roadside Safety Data Collection Plan*. Technical Report, Texas Transportation Institute, Texas A&M University System, College Station, Texas.
9. Mak, K.K., and Bligh, R.P. (1996) *Recovery-Area Distance Relationships for Highway Roadside*. Phase I Report, NCHRP Project G17-11.
10. Maycock, G., and Hall, R.D. (1984) *Accidents at 4-arm Roundabouts*. Transport and Road Research Laboratory Report 1120.
11. Miaou, S.-P., Hu, P.S., Wright, T., Davis, S.C., and Rathi, A.K. (1993) *Development of Relationship Between Truck Accidents and Geometric Design: Phase I*. FHWA-RD-91-124. FHWA, U.S. Department of Transportation.
12. Miaou, S.-P., and Lum, H. (1993) Modeling Vehicle Accidents and Highway Geometric Design Relationships. *Accident Analysis and Prevention*, 25(6):689-709.
13. Miaou, S.-P. (1994) The Relationship Between Truck Accidents and Geometric Design of Road Sections: Poisson Versus Negative Binomial Regressions. *Accident Analysis & Prevention*, 26(4): 471-482.
14. Miaou, S.-P. (1996) *Measuring the Goodness-of-Fit of Accident Prediction Models*. FHWA-RD-96-040. FHWA, U.S. Department of Transportation.
15. Miaou, S.-P. (1997) *An Extended Negative Binomial Regression Model: User Guide*. Oak Ridge National Laboratory, Oak Ridge, Tennessee.
16. Miaou, S.-P. (forthcoming) Estimating Vehicle Roadside Encroachment Frequencies Using Accident Prediction Models. *Transportation Research Record*. TRB, National Research Council, Washington, D.C..
17. Ray, M.H., Carney, III, J.F., and Opiela, K.S. (1995) Emerging Roadside Safety Issues, *TR News* 177, March-April.

18. Rodgman, E., Zegeer, C., and Hummer, J. (1989) *Safety Effects of Cross-Section Design for Two-Lane Roads - Data Base User's Guide*. Report submitted to FHWA, Revised, November.
19. Transportation Research Board (1987) *Designing Safer Roads^{3/4}Practices for Resurfacing, Restoration, and Rehabilitation*. Special Report 214 (Appendix F). National Research Council, Washington, D.C.
20. Viner, J.G. (1995) Rollovers on Sideslopes and Ditches. *Accident Analysis & Prevention*, 27(4): 483-491.
21. Zegeer, C.V., Hummer, J., Reinfurt, D., Herf, L., and Hunter, W. (1987) *Safety Effects of Cross-Section Design for Two-Lane Roads*. Volumes I and II. Chapel Hill: University of North Carolina.
22. Zegeer, C.V., Stewart, R., Reinfurt, D., Council, F., Neuman, T., Hamilton, E., Miller, T., and Hunter, W. (1990) *Cost-Effective Geometric Improvements for Safety Upgrading of Horizontal Curves*. Volume I. Final Report. Chapel Hill: University of North Carolina.

LIST OF TABLES

Table 1.	Simple kinematic equations used to estimate time to collision and impact speed for a given encroachment angle when encroachment trajectory is a straight line and deceleration rate is a constant	71
Table 2.	Estimated regression parameters of extended negative binomial regression models and associated statistics for guardrail accidents.....	72
Table 3.	Estimated regression parameters of extended negative binomial regression models and associated statistics for utility pole accidents.....	73

LIST OF FIGURES

Figure 1.	An overview of the encroachment-based approach.	74
Figure 2.	An example joint probability density function of encroachment speed and angle ...	75
Figure 3.	Impact envelope of a roadside object for a given vehicle encroachment angle.....	76
Figure 4.	Probability distributions of impact speeds as a function of the lateral offset of the object when an encroached vehicle is in the hazard envelope	77
Figure 5.	Probabilities of an encroached vehicle to hit point objects of different sizes at various lateral offsets.....	78
Figure 6.	Probabilities of an encroached vehicle to hit continuous objects of different lengths at various lateral offsets	79
Figure 7.	Probabilities of an encroached vehicle to collide with a point object and a continuous object at a speed greater than v	80
Figure 8.	Comparison of the roadside encroachment frequency estimated from the accident prediction model developed in this study and observed frequencies from earlier studies.....	81
Figure 9.	Roadside encroachment frequencies estimated from two utility pole accident models under three different sizes of hazard envelopes.....	82

Table 1. Simple kinematic equations used to estimate time to collision and impact speed for a given encroachment angle when encroachment trajectory is a straight line and deceleration rate is a constant.

Condition	Time to Collision, t_c	Impact Speed, v_c
if $d_c \leq v_0 t_r$	$t_c = d_c / v_0$	$v_c = v_0$
if $v_0 t_r < d_c \leq v_0 t_r + (v_0^2 / 2D)$	$t_c = t_r + v_0 / D$ $- \left\{ v_0^2 - 2D[d_c - v_0 t_r] \right\}^{1/2} / D$	$v_c = \left\{ v_0^2 - 2D[d_c - v_0 t_r] \right\}^{1/2}$
if $d_c > v_0 t_r + (v_0^2 / 2D)$	$t_c = \text{N/A}$ (i.e., no collision)	$v_c = \mathbf{0}$

Notations:

d_c : encroachment distance to collision (mi or km) (see the notes below)

D_{obj} : lateral offset of the object (mi or km), measured from the outside edge of travelway (see Figure 3)

v_0 : encroachment speed (mi/hr or km/hr)

v_c : impact speed (mi/hr or km/hr)

f : encroachment angle (degree)

t_r : driver's response delay (sec), measured from the time encroachment occurs until the driver applies the brake

D : constant deceleration rate (mi/sec² or km/sec²), e.g., 0.5g (=0.5x32.2/5280 mi/sec²=0.00304 mi/sec²=0.00304x3600² mi/hr²=39,518 mi/hr²); D actually depends on surface type, sideslope, and wetness.

Notes:

From Figure 3, the distance that a vehicle needs to travel to collide with the object after encroachment can be estimated as

$$d_c = \frac{D_{obj}}{\sin(f)} \quad \text{if the encroachment occurs in zones 1 and 2;}$$

and, depending on where the encroachment occurs within zone 3, the distance is between

$$d_c = \frac{D_{obj}}{\sin(f)} \quad \text{and} \quad d_c = \frac{D_{obj} + W_{obj}}{\sin(f)}$$

Strictly speaking, it also depends on vehicle orientation at the time of collision. The two equations above suggest that $D_{obj} / \sin(f)$ is a good estimate of the distance only when $D_{obj} \gg W_{obj}$ or when continuous objects are considered where $\ell_{obj} \gg W_{obj}$ and f is not too small (i.e., the hazard envelope of zone 3 is considerably smaller than that of zones 1 and 2 combined).

Unit conversions: 1 mi = 5,280 ft = 1.6 km = 1,600 m

Table 2. Estimated regression parameters of extended negative binomial regression models and associated statistics for guardrail accidents.

Covariate	Estimated NB Model Parameters			
	Guardrail Length > 0.1 mi (n=272 Sections)	Guardrail Length > 0.15 mi (n=217 Sections)		Guardrail Length > 0.2 mi (n=188 Sections)
Dummy intercept (=1): the associated parameter is b_1 , as described in the text	1.66290 (0.229; 7.26)	1.39974 (0.241; 5.81)	1.41633 (0.233; 6.08)	1.18578 (0.253; 4.69)
AADT per lane (10^3 vehicles per day per lane)	-0.20515 (0.095; -2.16)	-0.18061 (0.096; -1.89)	-0.18278 (0.096; -1.91)	-0.12887 (0.099; -1.30)
Lane width (ft)	----	----	----	----
Horizontal curvature (degrees/100 ft arc)	----	----	----	----
Vertical grade (percent)	----	----	----	----
Clear zone width (ft): Paved shoulder width	-0.18391 (0.034; -5.42)	-0.18086 (0.035; -5.22)		-0.17611 (0.035; -5.00)
Clear zone width (ft): Unpaved shoulder width (i.e., earth, grass, gravel, or stabilized shoulder width)	-0.17013 (0.040; -4.26)	-0.14890 (0.040; -3.70)		-0.12390 (0.043; -2.90)
Clear zone width (ft): Additional clear zone width beyond shoulders	-0.27137 (0.077; -3.53)	-0.19977 (0.076; -2.62)		-0.20993 (0.079; -2.64)
Clear zone width (ft): Total available width	----	----	-0.17363 (0.033; -5.32)	----
Dispersion parameter of the NB model	0.89325 (0.155; 5.77)	0.79412 (0.152; 5.22)	0.79904 (0.153; 5.22)	0.75785 (0.153; 4.95)
Log-likelihood function/n	-1.64	-1.71	-1.72	-1.72
Akaike Information Criterion Value/n	3.33	3.48	3.47	3.50
Expected vs. Observed total number of accidents	508 vs. 450	430 vs. 397	430 vs. 397	380 vs 360

Notes: (1) About five years of accident data (1980-1984) were available. (2) Values in parentheses are asymptotic standard deviation and t-statistics of the estimated parameters above. (3) ----- indicates "not selected in the final model." (4) The exposure measure, vehicle-miles traveled, in the model is in million vehicle-miles. (5) 1 mi = 1.61 km and 1 ft = 0.3048 m.

Table 3. Estimated regression parameters of extended negative binomial regression models and associated statistics for utility pole accidents.

Covariate	Estimated NB Model Parameters		
Dummy intercept (=1): the associated parameter is b_1 and, as described in the text, $d = 168$ ft	0.68440 (0.264; 2.59)	0.68438 (0.266; 2.57)	1.97345 (1.020; 1.94)
AADT per lane (10^3 vehicles per day per lane)	-0.30398 (0.073; -4.14)	-0.38470 (0.071; -5.39)	-0.38376 (0.071; -5.37)
Lane width (ft)	----	----	----
Horizontal curvature (degrees/100 ft arc)	----	----	----
Vertical grade (percent)	----	----	----
Sideslope (e.g., 3:1 and 7:1 slopes are recorded as $1/3=0.33$ & $1/7=0.14$, respectively.)	----	----	----
Clear zone width (ft): Paved shoulder width	-0.15338 (0.035; -4.44)	----	-----
Clear zone width (ft): Earth, grass, gravel, or stabilized shoulder width	-0.18211 (0.027; -6.69)	----	-----
Clear zone width (ft): Additional clear zone width beyond shoulders	-0.05198 (0.015; -3.54)	----	-----
Clear zone width (ft): Total available width	----	-0.08101 (0.014; -5.82)	-0.27419 (0.151; -1.82)
Clear zone width > 10.5 ft (ft): Clear zone width, if it is greater than 10.5 ft; 0 otherwise	----	----	0.10819 (0.088; 1.23)
Clear zone width > 20.5 ft (ft): Clear zone width, if it is greater than 20.5 ft; 0 otherwise	----	----	0.037183 (0.035; 1.06)
Dispersion parameter of the NB model	0.40907 (0.191; 2.14)	0.60062 (0.206; 2.91)	0.58807 (0.204; 2.87)
Loglikelihood function/n	-0.69	-0.71	-0.70
Akaike Information Criterion Value/n	1.40	1.42	1.42
Expected vs. observed total number of accidents	305 vs. 293	309 vs 293	308 vs. 293

Notes: (1) 855 road sections were used in developing these models (i.e., $n=855$). (2) The average pole spacing of each road section is greater than 0.1 mi. (3) About five years of accident data (1980-1984) were used. (4) Values in parentheses are asymptotic standard deviation and t-statistics of the estimated parameters above; (5) ---- indicates “not selected in the final model.” (6) The exposure measure, vehicle-miles traveled, in the model is in million vehicle-miles. (7) 1 mi = 1.61 km and 1 ft = 0.3048 m

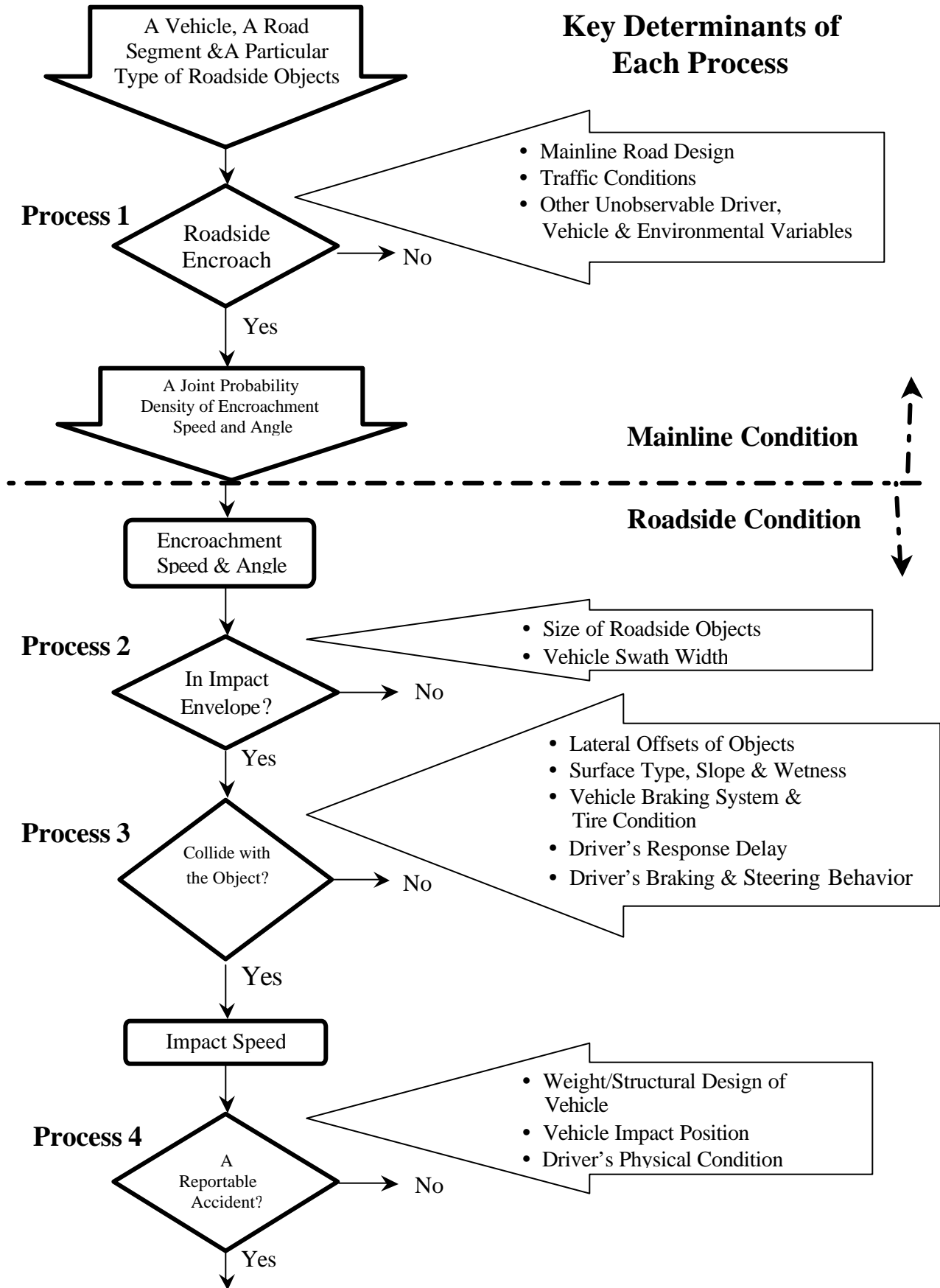


Figure 1. An overview of the encroachment-based approach.

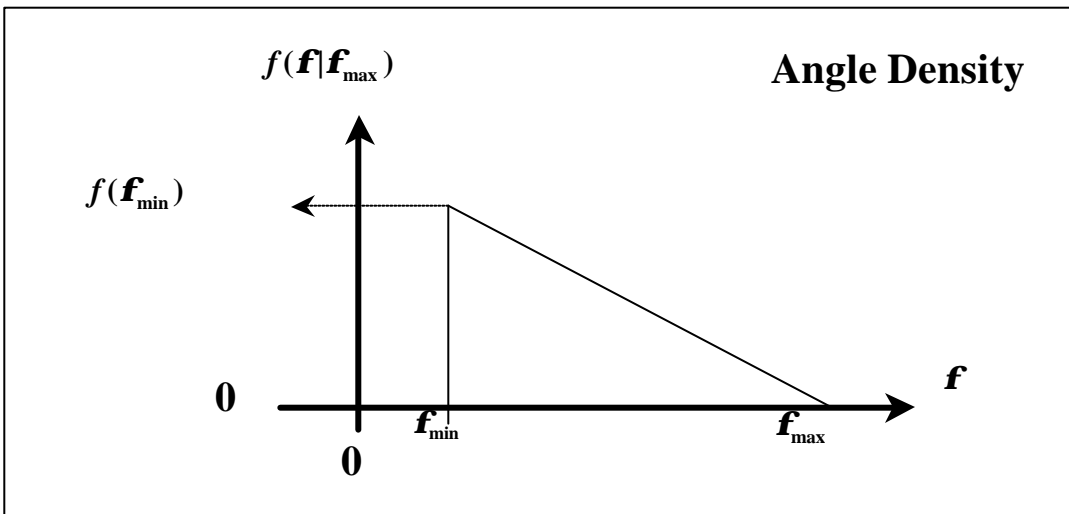
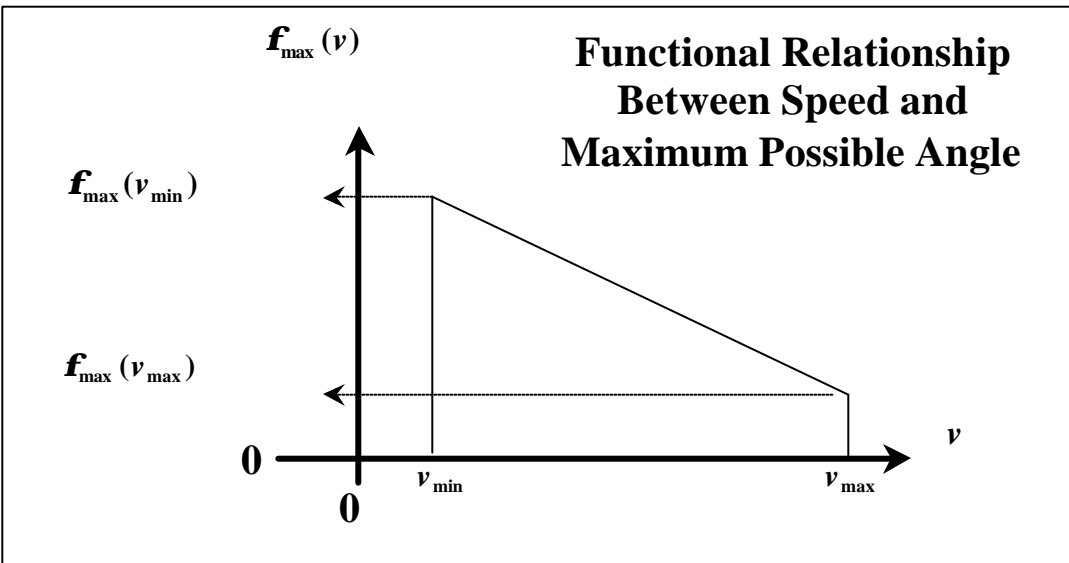
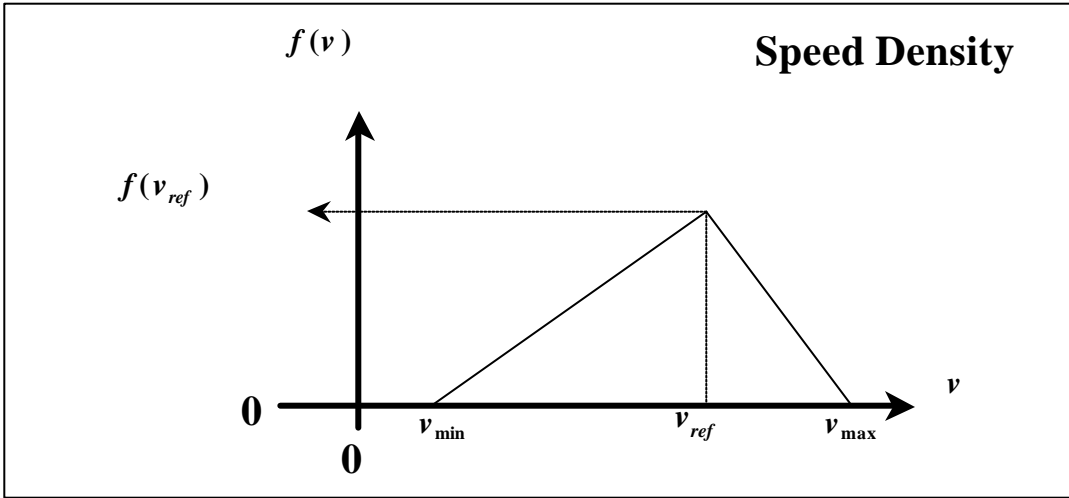


Figure 2. An example joint probability density function of encroachment speed and angle.

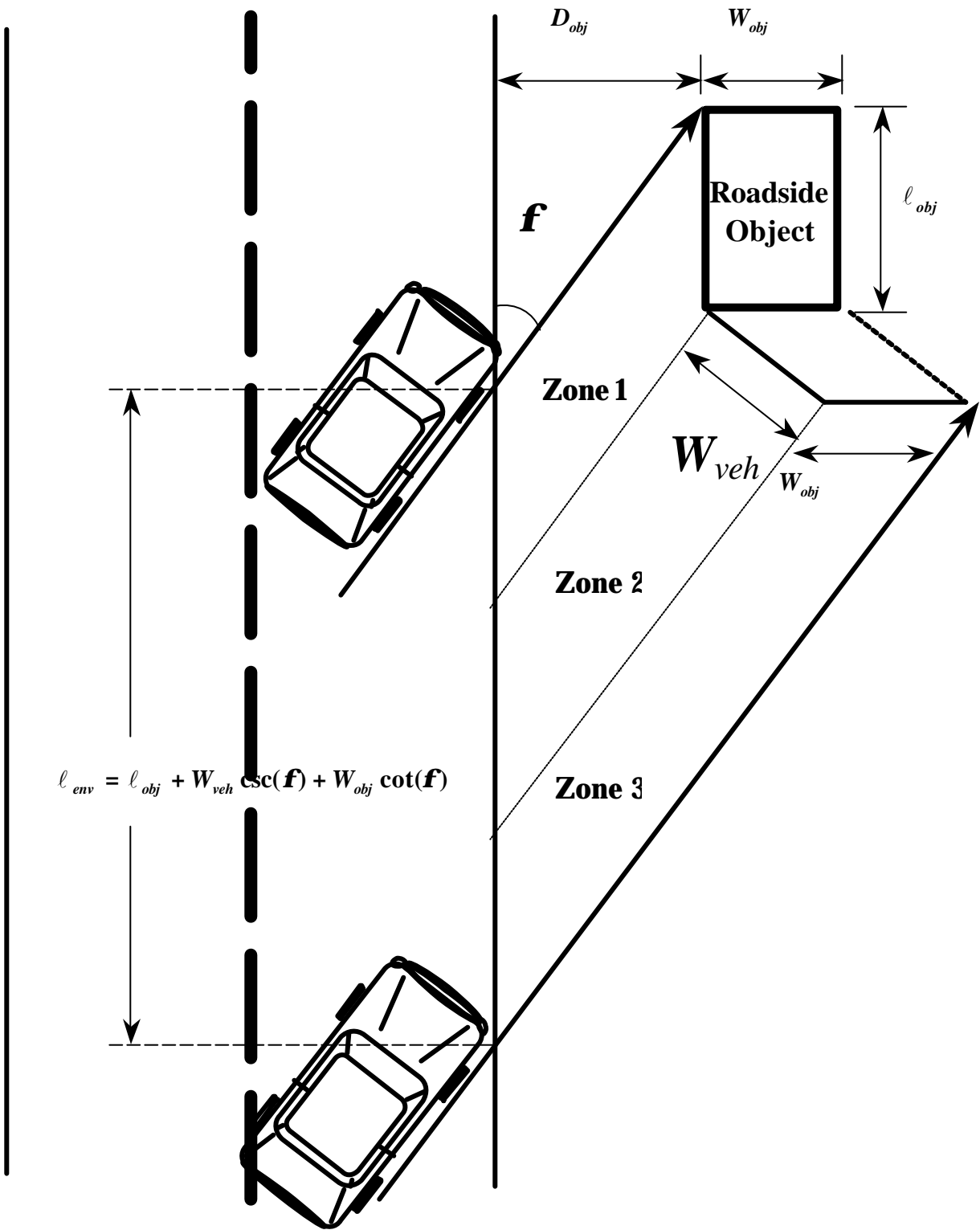


Figure 3. Impact envelope of a roadside object for a given vehicle encroachment angle.

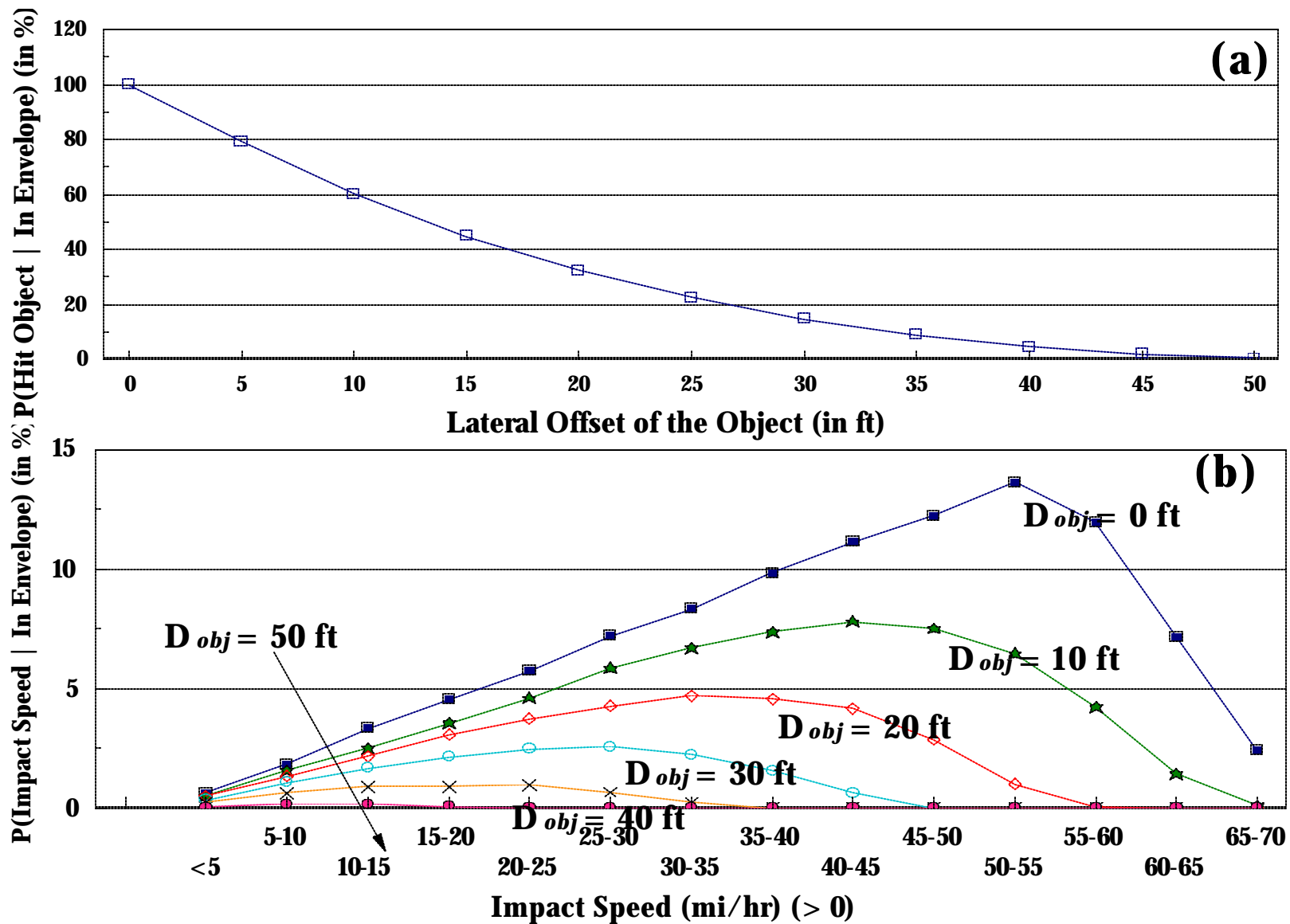


Figure 4. Probability distributions of impact speeds as a function of the lateral offset of the object when the encroached vehicle is in the hazard envelope.

(1 mi = 1.61 km, 1 ft = .305 m, 1 in = 25.4 mm)

P(Hit Object | Encroachment) (%)

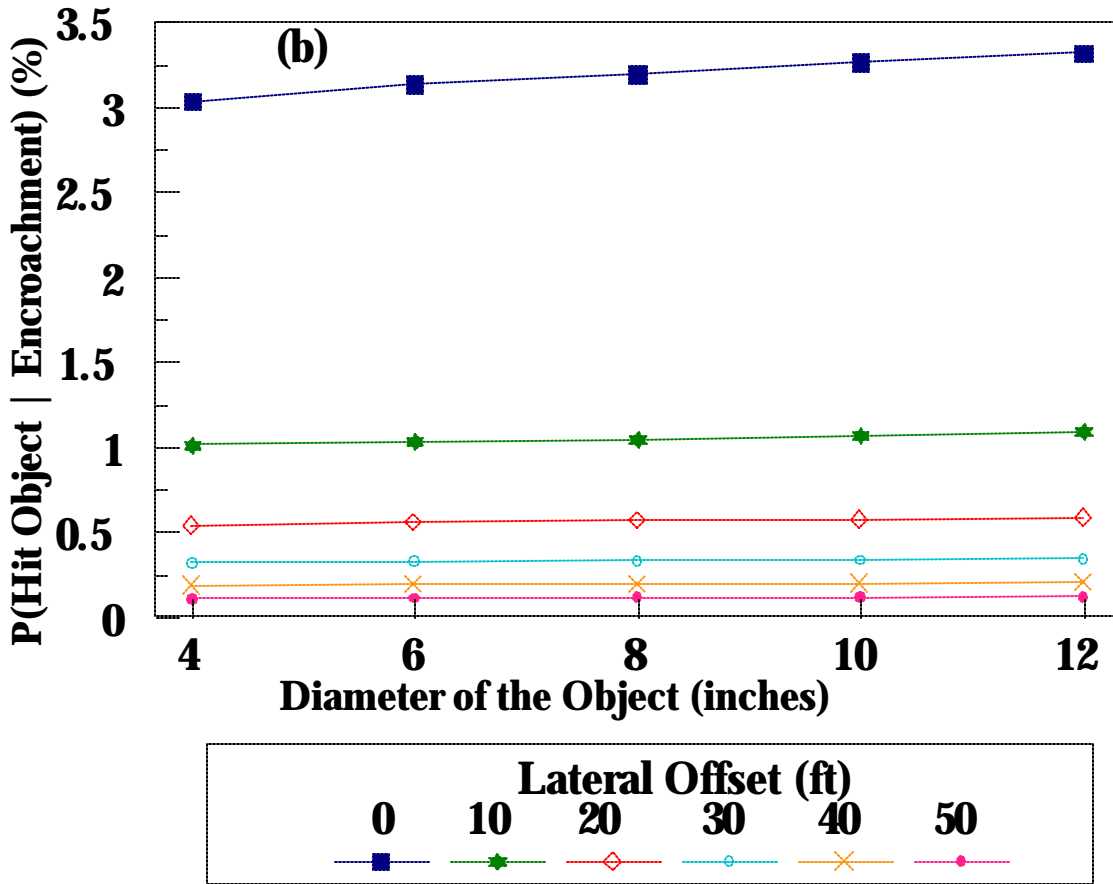
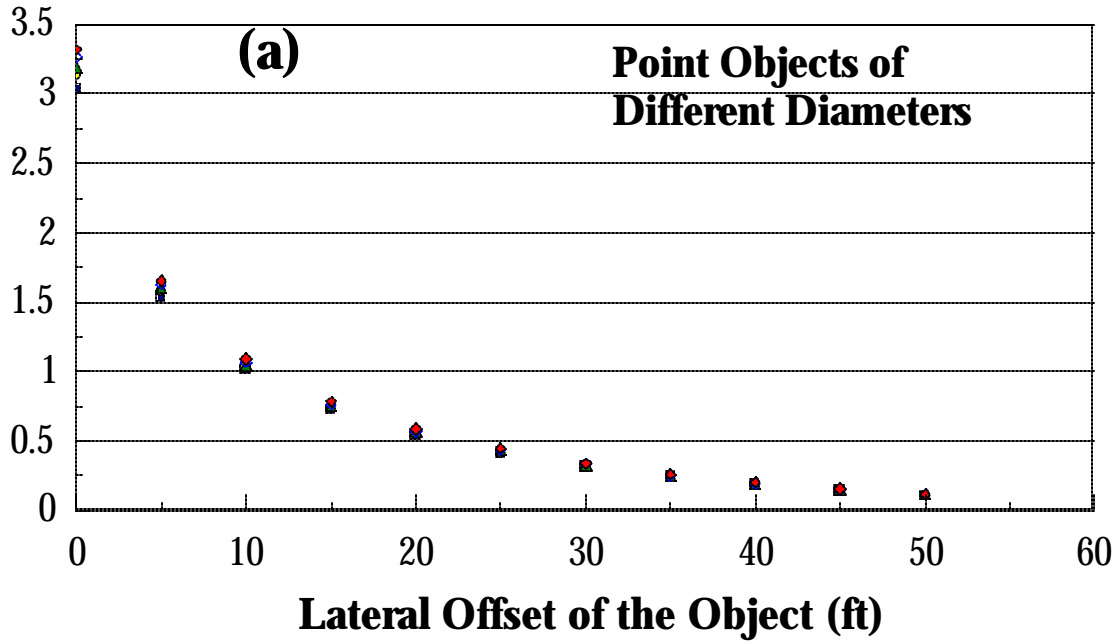


Figure 5. Probabilities of an encroached vehicle to hit point objects of different sizes at various lateral offsets.

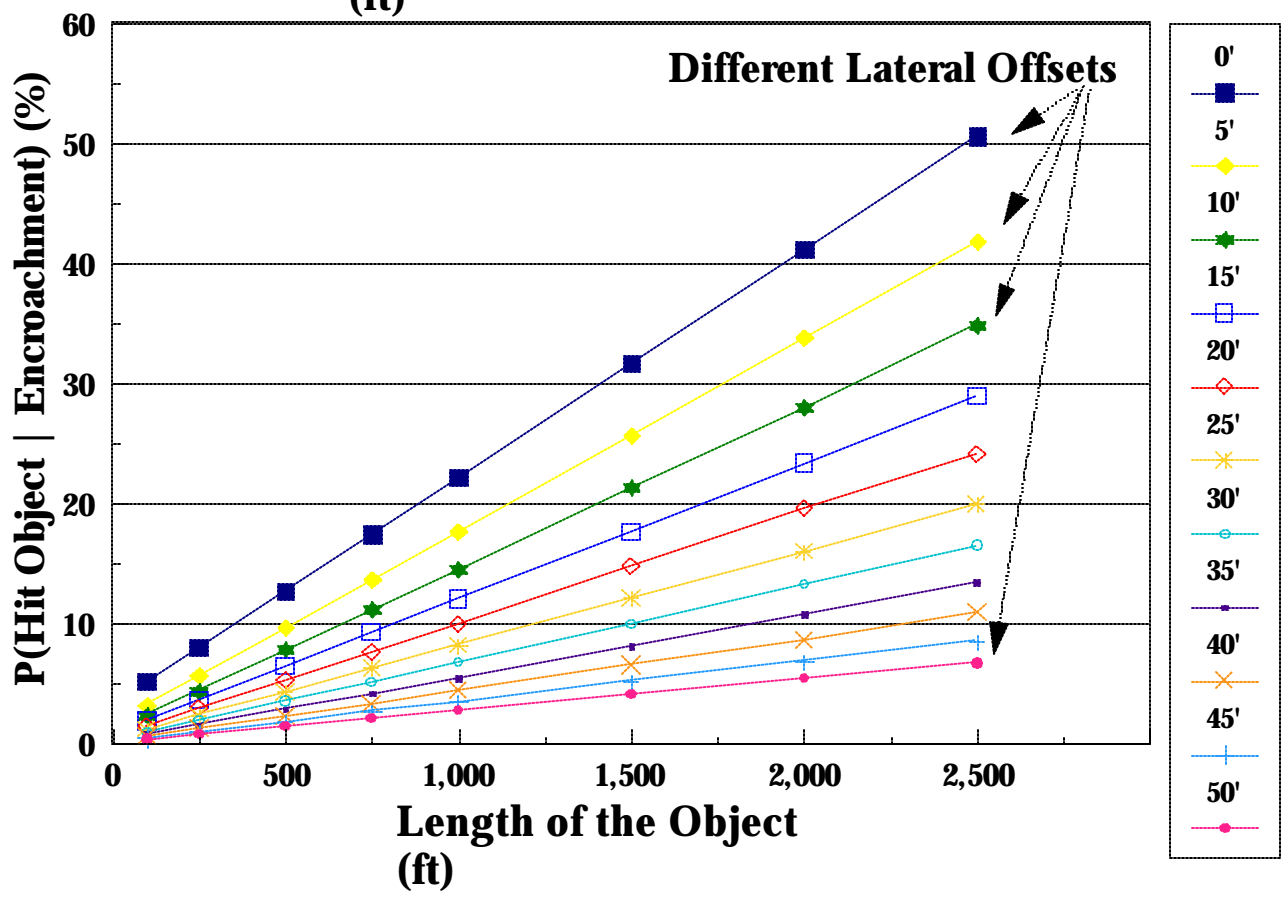
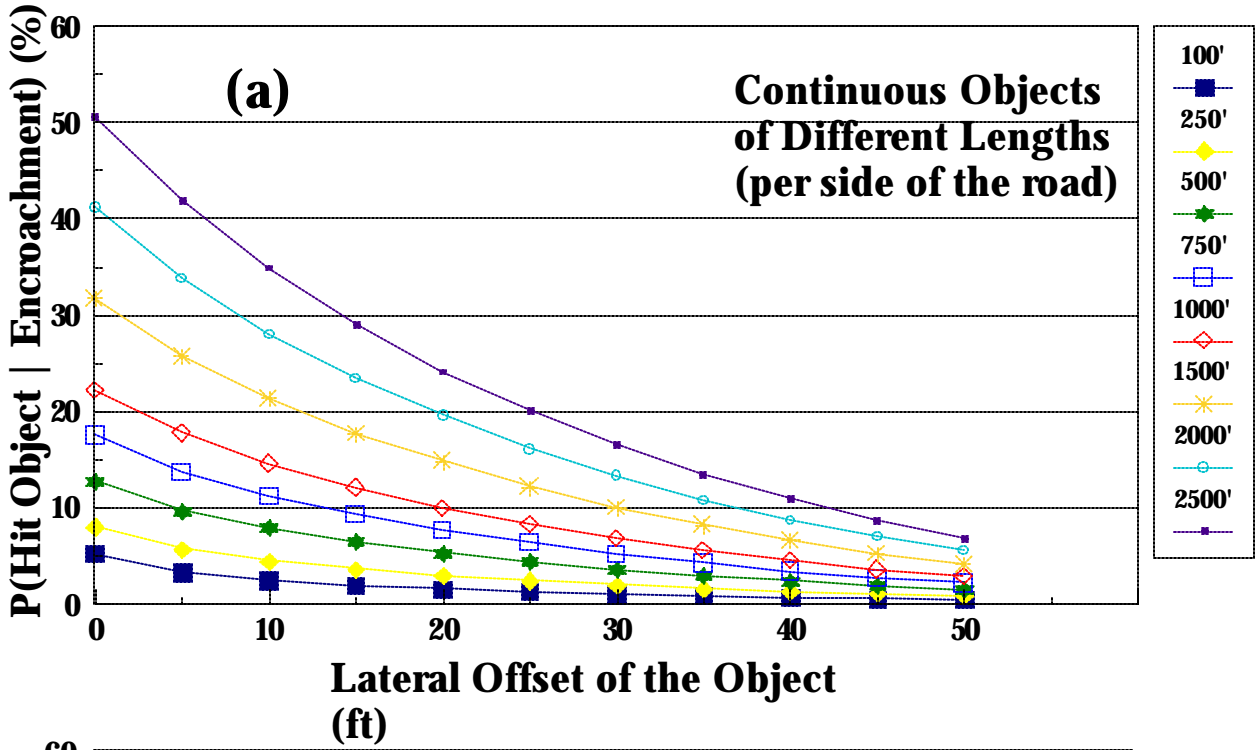


Figure 6. Probabilities of an encroached vehicle to hit continuous objects of different lengths at various lateral offsets.

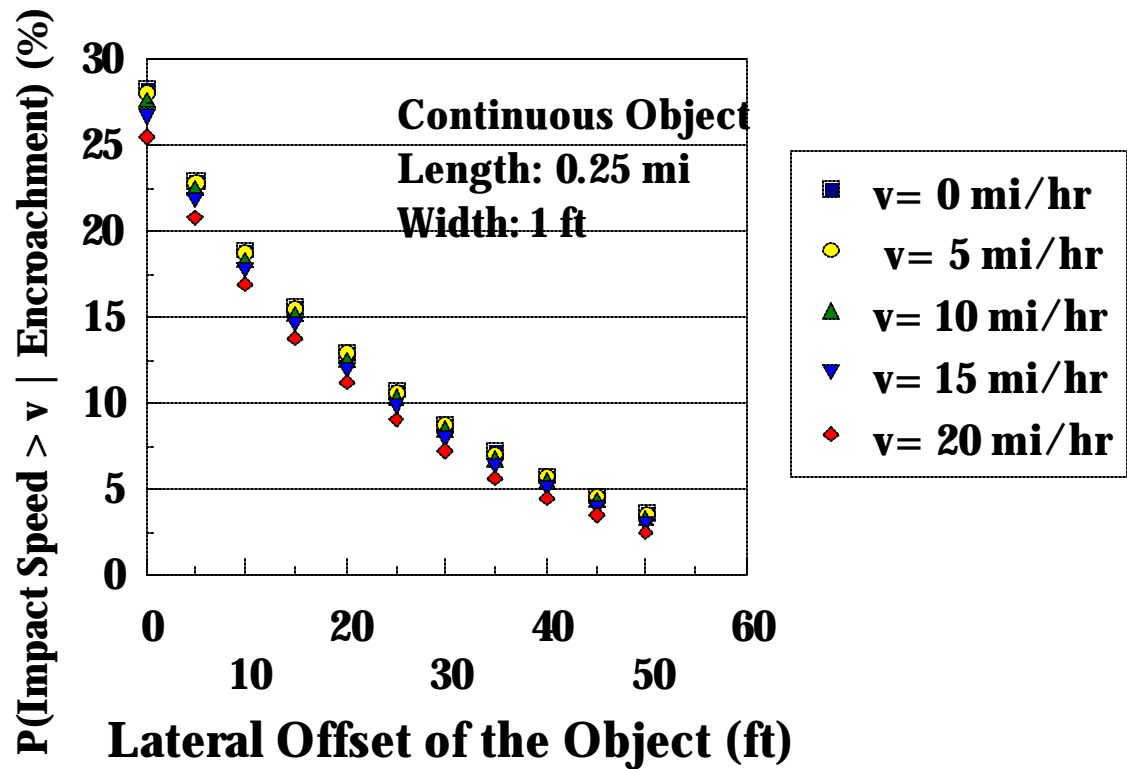
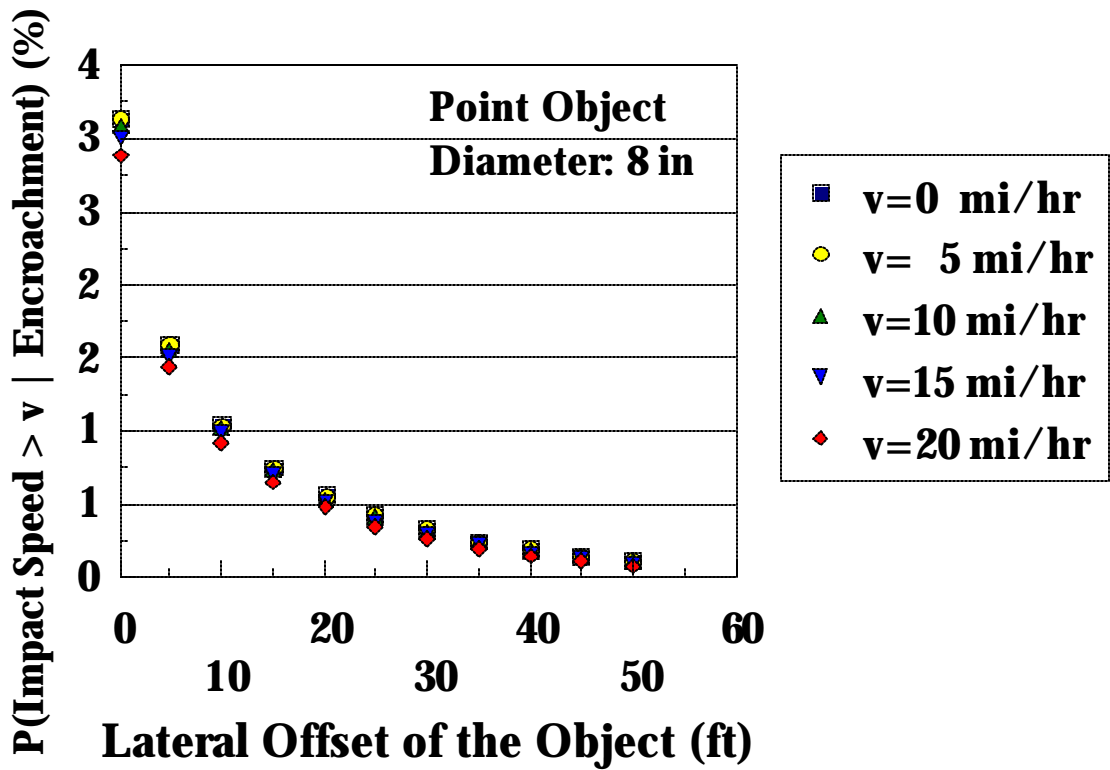


Figure 7. Probabilities of an encroached vehicle to collide with a point object and a continuous object at a speed greater than v.

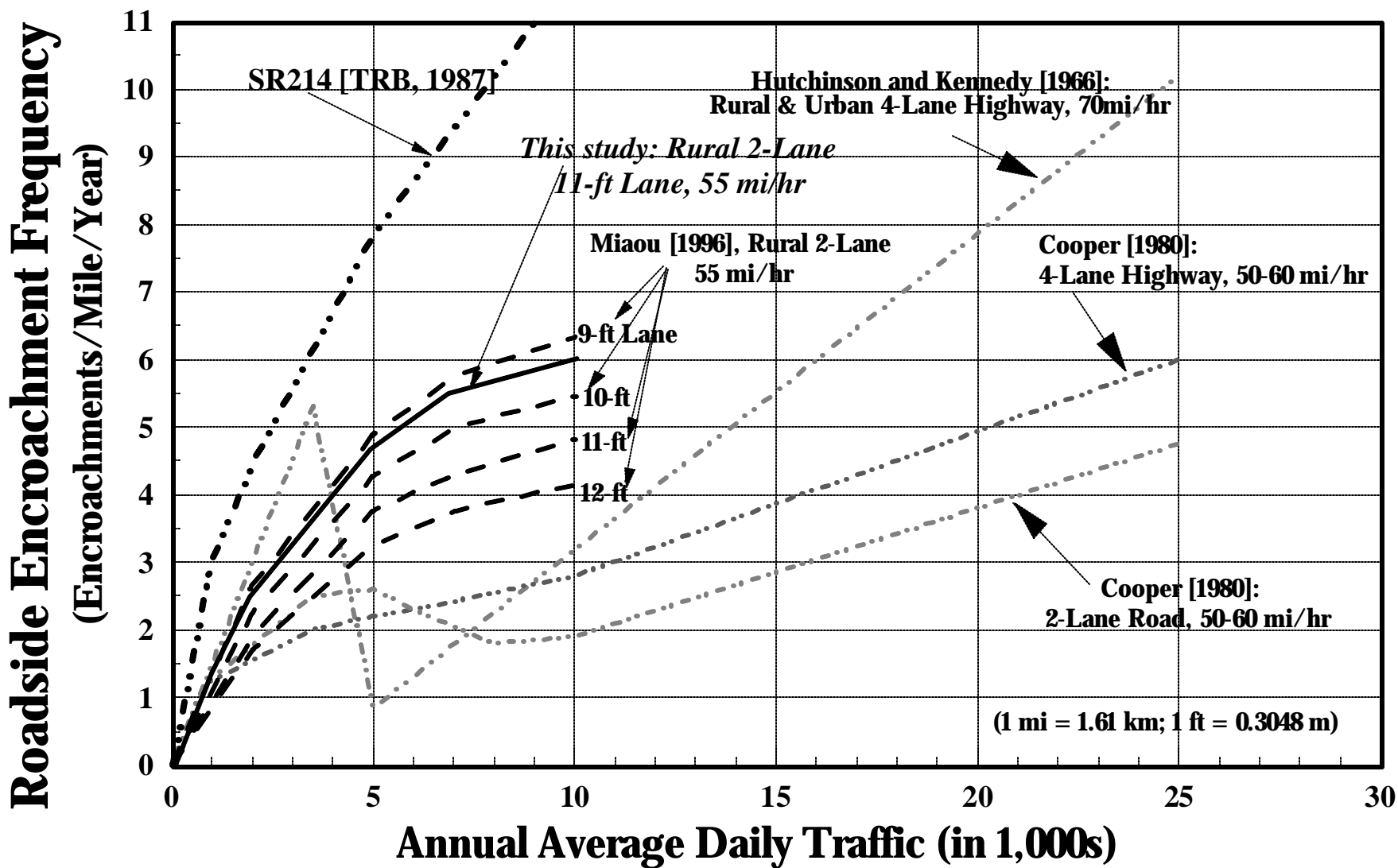


Figure 8. Comparison of the roadside encroachment frequency estimated from the accident prediction model developed in this study and observed frequencies from earlier studies.

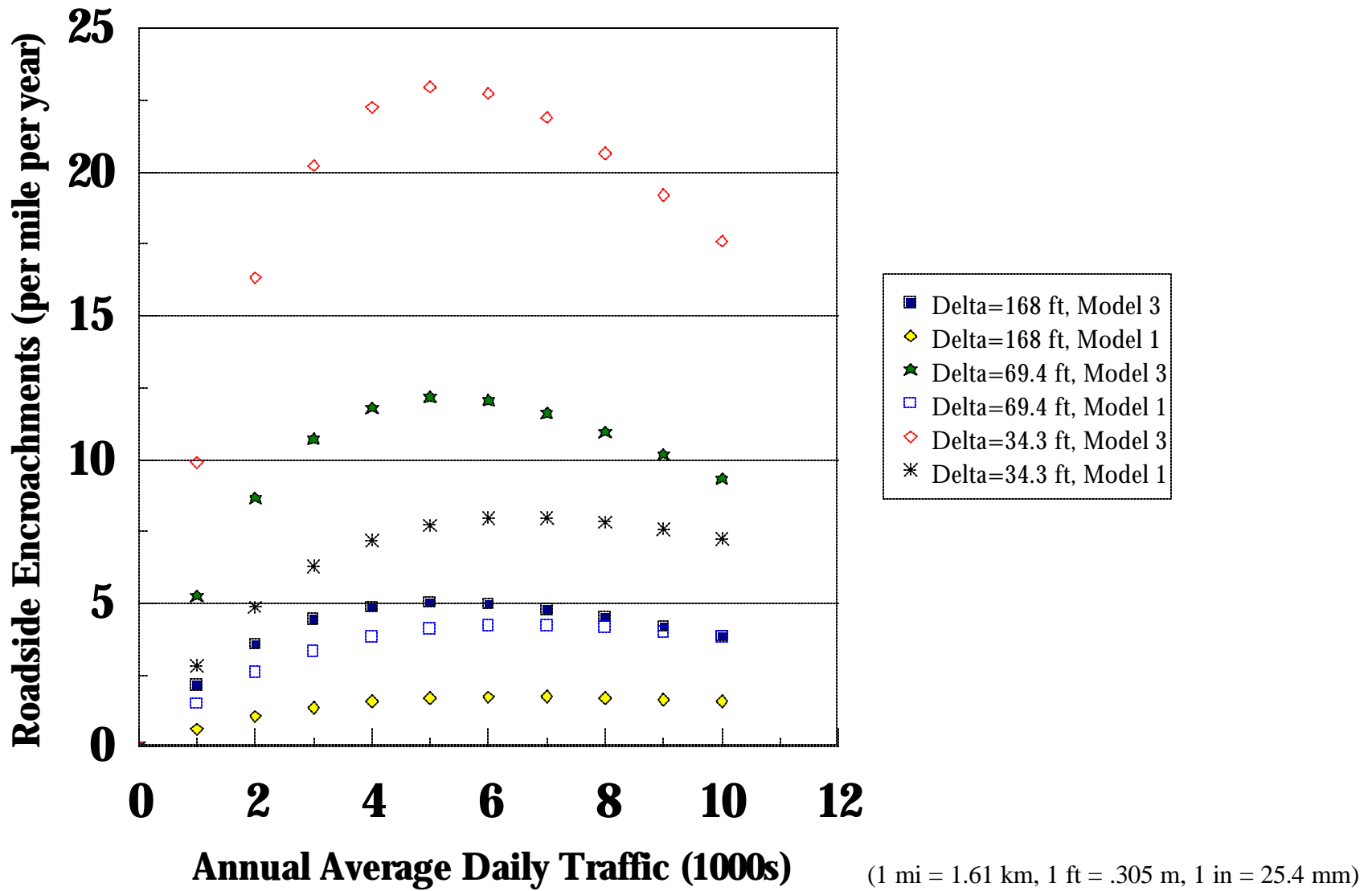


Figure 9. Roadside encroachment frequencies estimated from two utility pole accident models under three different sizes of hazard envelopes.

APPENDIX C

RESEARCH STATEMENT

ESTIMATING ROADSIDE ENCROACHMENT RATES WITH THE COMBINED STRENGTHS OF ACCIDENT- AND ENCROACHMENT-BASED APPROACHES

Prepared by
Shaw-Pin Miaou, Ph.D.
Center for Transportation Analysis
Oak Ridge National Laboratory
October 24, 1997

BACKGROUND

Models used in previous studies to quantify the relationships between run-off-the-road (ROR) accidents and roadside hazards, such as utility poles, trees, guardrail, median barriers, and embankments, have been categorized as using either an accident-based approach or an encroachment-based approach. The former, which uses the Poisson and negative binomial (NB) types of regression models, has a solid statistical ground, but has been criticized as being overly empirical and lacking engineering basis. The latter, on the other hand, has analytical and engineering strengths, but has been described as being full of subjective assumptions and lacking sufficient supporting data. Historically, researchers on roadside safety seem to have treated the accident-based and encroachment-based approaches as two competing, disconnected approaches and seldom or never attempt to seek the opportunity to combine the strengths of both.

In the last 15 years or so, despite its limitations, encroachment-based cost-effectiveness procedures have gained increasing application in determining the need for roadside safety improvements and for developing general selection guidelines for roadside safety hardware. Some procedures have been adopted as part of the AASHTO's roadside design guideline [AASHTO, 1989]. More importantly, the approach will form the basis of the roadside model in the Accident Analysis Module (AAM) of the Interactive Highway Safety Design Model (IHSDM) that is currently being developed by the Federal Highway Administration (FHWA) [Griffith and Bared, 1997].

Vehicle roadside encroachment characteristics, including the encroachment rate or encroachment probability, are key input parameters to the encroachment-based cost-effectiveness procedures.

The reliability of the results from the procedures is directly affected by the quality of these input parameters. At present, it appears that available encroachment data to estimate these input parameters are extremely limited and largely outdated--some were collected over 30 years ago on a small number of road sections. The FHWA and Transportation Research Board (TRB) have been addressing the requirements and collection of such data through their sponsorship of several roadside safety projects. As a result, rather comprehensive data collection plans have been proposed, and results of pilot data collection efforts have been reported [Mak and Sicking, 1992; Daily et al., 1997; Mak and Bligh, 1996]. A review of these plans and pilot data collection results suggests that the cost of collecting the required roadside field data will be very high. Furthermore, the validity of any field-collected encroachment data may be questionable because of the technical difficulty in distinguishing between controlled (or intentional) and uncontrolled (or unintentional) encroachments.

In two recent studies by Miaou [1996 and August, 1997], he proposed a method to estimate roadside encroachment rates using accident-based models. The method combines the strengths of both the accident-based and encroachment-based approaches. Specifically, it incorporates the analytical and engineering strengths of the encroachment-based models into the formulation of the mean function of accident-based models. Note that the mean function in accident-based regression models specifies the functional relationship between the expected accident rate and covariates (or independent variables). Miaou further illustrated the use of such a method to estimate roadside encroachment rates for rural two-lane, undivided roads using data from the FHWA Seven States Cross-Section Data Base [Rodgman et al., 1989].

Three illustrations have been conducted in Miaou's studies. In the first illustration, all ROR accidents were considered. Among other mainline design and traffic variables, general roadside hazard indices which include sampling distributions of clear zone width and sideslope along each road section were used in developing ROR accident-based prediction models. In the second and third illustrations, accidents involving a specific type of roadside hazards were considered. Specifically, guardrail and utility pole accidents were considered in the second and third illustrations, respectively. The lateral offset of individual roadside hazards was the main roadside design variable considered in developing models. The estimated roadside encroachment

rates were found to be consistent among the three illustrations and compatible with those estimated by earlier encroachment-based studies in terms of their order of magnitude. These results indicate that the proposed method can be a viable approach to estimating encroachment rates without actually collecting the encroachment data that can be expensive and technically difficult.

At the conceptual and analytical levels, the strengths of the proposed method can be summarized as follows:

- (1) It is straightforward to estimate encroachment rates for various mainline design and traffic conditions, e.g., for different lane width, horizontal curvature, vertical grade, and traffic volumes, provided that adequate mainline data are available to develop the accident-based model. To actually collect such detailed encroachment data will be very expensive and may not even be practical.
- (2) When good roadside accident history is available for individual sites, *site-specific* encroachment rates can potentially be obtained with the proposed method by using the Empirical Bayes (EB) method. This allows site-specific driver, vehicle, and environmental factors that are not available in developing accident-based models to be reflected in an objective way in the final encroachment rate estimate. (Note that this cannot be done in any objective way with the current encroachment-based methods.) Since the roadway model in the AAM of IHSDM will use EB estimator when accident history is available for individual sites [Griffith and Bared, 1997], this strength of the proposed method enables the roadway and roadside models to adopt the same statistical estimation procedure and, therefore, it will increase the probability of obtaining consistent estimates from the two models within the AAM.
- (3) Provided a flexible mean functional form is used in developing accident-based models, the encroachment rates estimated from the proposed method are relatively unaffected by the underreporting of minor accidents. This strength has been explained in two different ways in the two studies by Miaou [1996 and August 1997], one of which used encroachment-based approach to illustrate this point.
- (4) The estimated encroachment rate is based on ROR accident data and is, therefore,

uncontaminated by controlled encroachments. Unlike field-collected encroachment data, there is no need to develop a procedure to distinguish between controlled and uncontrolled encroachments (which can be subjective and technically challenging).

- (5) Standard statistical inferences, especially the sampling error (or sampling variability), can be readily provided for the estimated encroachment rates. (Note, however, that the generation of these inferences can be computationally intensive.)
- (6) Because accident, traffic, and roadway data, such as those contained in the Highway Safety Information System (HSIS), are constantly being collected, updated, and maintained. The estimated encroachment rates can be updated frequently, if necessary, using the latest data with a marginal cost.
- (7) In the proposed method, the formulation of the mean function in developing the accident-based model (an NB regression-based model) takes into account the analytical procedure used in the encroachment-based model which is guided by driver behavior, vehicle dynamics, and traffic flow theories. This approach to formulation, again, increases the chance of obtaining consistent estimates of roadway and roadside accident rates from the roadway and roadside models in the AAM of the IHSDM.

Despite these conceptual and analytical strengths, the consistency of the proposed method has only been illustrated using the data from one data base. In addition, the accident data contained in the data base are not up-to-date (from 1980 to 1984). It is important that the consistency of the proposed method be “validated” with independent and more up-to-date data sets. A research plan to “validate” the proposed method is described in the following section.

PROPOSED RESEARCH PLAN

We propose that the consistency of Miaou’s method be “validated” with Minnesota and Washington data from the HSIS. Specifically, the data sets to be employed are those used by Bared and Vogt [1997] in developing rural two-lane roadway models for the AAM. They have developed promising NB regression models for total road segment accidents using these two data sets. Their models are considered quite complete in terms of the number and type of geometric design variables that are included in the model and are up-to-date in terms of the accident data considered. Because roadside data are generally not available in State road inventory data base,

most of the roadway models developed by previous studies did not consider roadside variables. An important feature of Bared and Vogt's model is that it includes a general roadside hazard index, called roadside hazard rating, which were collected from a video-log system maintained at FHWA. Because Bared and Vogt's models are quite promising, they are likely to be adopted as the "base roadway model" in the AAM for a typical (or ideal) design and for establishing accident modification factors for alternative designs.

In the light of these developments in roadway models, there are several advantages of "validating" Miaou's method with these two data sets:

- (1) The roadside hazard rating, as collected by Bared and Vogt, can be readily used in "validating" the method without new roadside data collection effort.
- (2) The data have been quality checked by Bared and Vogt, which will increase the chance of developing good encroachment rate estimates and will reduce data preparation cost.
- (3) If Bared and Vogt's models are adopted as part of the roadway model of AAM, then using the same data sets (as those used by Bared and Vogt) to develop the encroachment rates for roadside models will increase the probability of obtaining consistent roadway and roadside estimates from the two models.

PROPOSED TASKS

The specific tasks to be conducted under this plan include:

Task A: Obtain and review MN and WA data.

Task B: Prepare the data in a suitable format for developing accident prediction models.

Task C: Develop accident prediction models using MN and WA data.

Because accident types are organized differently in Washington and Minnesota, it may not be meaningful to develop one combined model for run-off-the-road accidents for the two States. In this task, we will try to build models for each State and study the feasibility of developing a combined model for the two States. The extended NB regression model developed by Miaou will be used in this study.

Task D: Estimate roadside encroachment rates.

If reasonable accident prediction models are developed in Task C, roadside encroachment rates will be generated using the accident prediction model proposed by Miaou [1996 and August 1997]. And, if feasible, these rates will be generated by AADT, lane width, horizontal curvature, and vertical grade.

Task E: Develop encroachment adjustment factors for horizontal curvature and vertical grade.

Task F: Prepare a draft report to summarize the study.

Task G: Prepare a final report.

REFERENCES

1. American Association of State Highway and Transportation Officials (AASHTO) (1989) *Roadside Design Guide*. Washington, D.C.
2. Bared, J.G. and Vogt, A. (1997) Accident Models for Two-Lane Rural Highways. Paper submitted to Transportation Research Board (TRB) for presentation in the 77th TRB Annual Meeting and for publication in Transportation Research Record.
3. Daily, K., Hughes, W., and McGee, H. (1997) *Experimental Plans for Accident Studies of Highway Design Elements: Encroachment Accident Study*. FHWA-RD-96-081. FHWA, U.S. Department of Transportation.
4. Griffith, M.S., and Bared, J.G. Overview of the Accident Analysis Module of the Interactive Highway Safety Design Model. Unpublished paper. Federal Highway Administration, June 3, 1997.
5. Mak, K.K., and Sicking, D.L. (1992) *Development of Roadside Safety Data Collection Plan*. Technical Report, Texas Transportation Institute, Texas A&M University System, College Station, Texas.
6. Mak, K.K., and Bligh, R.P. (1996) *Recovery-Area Distance Relationships for Highway Roadsides*. Phase I Report, NCHRP Project G17-11.
7. Miaou, S.-P. (1996) *Measuring the Goodness-of-Fit of Accident Prediction Models*. FHWA-RD-96-040. FHWA, U.S. Department of Transportation.
8. Miaou, S.-P. Another Look at the Relationship Between Accident- and Encroachment-Based Approaches to Run-Off-the-Road Accidents Modeling. Working Paper. Center for Transportation Analysis, Oak Ridge National Laboratory, Oak Ridge, Tennessee, August 1997.
9. Rodgman, E., Zegeer, C., and Hummer, J. (1989) *Safety Effects of Cross-Section Design for Two-Lane Roads - Data Base User's Guide*. Report submitted to FHWA, Revised, November.